J Nonlinear Sci (2010) 20: 425–461
DOI 10.1007/s00332-010-9064-z

Journal of Nonlinear Science

A System of ODEs for a Perturbation of a Minimal Mass Soliton

Jeremy L. Marzuola · Sarah Raynor · Gideon Simpson

Received: 7 May 2009 / Accepted: 1 March 2010 / Published online: 17 April 2010

Abstract We study soliton solutions to the nonlinear Schrödinger equation (NLS) with a saturated nonlinearity. NLS with such a nonlinearity is known to possess a minimal mass soliton. We consider a small perturbation of a minimal mass soliton and identify a system of ODEs extending the work of Comech and Pelinovsky (Commun. Pure Appl. Math. 56:1565–1607, 2003), which models the behavior of the perturbation for short times. We then provide numerical evidence that under this system of ODEs there are two possible dynamical outcomes, in accord with the conclusions of Pelinovsky et al. (Phys. Rev. E 53(2):1940–1953, 1996). Generically, initial data which supports a soliton structure appears to oscillate, with oscillations centered on a stable soliton. For initial data which is expected to disperse, the finite dimensional dynamics initially follow the unstable portion of the soliton curve.

Communicated by M.I. Weinstein.

J.L. Marzuola
Department of Applied Mathematics, Columbia University, 200 S. W. Mudd, 500 W. 120th St., New York City, NY 10027, USA
e-mail: jm3058@columbia.edu

S. Raynor (✉)
Mathematics Department, Wake Forest University, P.O. Box 7388, 127 Manchester Hall, Winston-Salem, NC 27109, USA
e-mail: raynorsg@wfu.edu

G. Simpson
Mathematics Department, University of Toronto, 40 St. George St., Toronto, Ontario M5S 2E4, Canada
e-mail: simpson@math.toronto.edu

Keywords NLS · Nonlinear Schrödinger equation · Orbital stability · Solitons · Effective dynamics

Mathematics Subject Classification (2000) 35C08 · 35B35 · 35Q55

1 Introduction

The nonlinear Schrödinger equation (NLS) in $\mathbb{R}^d \times \mathbb{R}^+$:

$$iu_t + \Delta u + g\big(|u|^2\big)u = 0, \qquad u(x,0) = u_0(x) \tag{1.1}$$

emerges as a leading order description of important physical systems in optics, many body quantum systems, hydrodynamics, and plasma physics. Moreover, it is a canonical equation demonstrating the competition between nonlinearity and dispersion.

In many applications, the leading order approximation of the nonlinearity, $g(s)$, is the power nonlinearity $g(s) = \pm s^\sigma$. For example, $g(s) = s$, yields the focusing cubic NLS equation. Cubic NLS appears in many contexts, including many body quantum systems, when the Hartree equation is approximated with pairwise delta function interactions. It similarly appears in nonlinear optics if the higher order corrections to the nonlinear index of refraction are neglected.

Such approximations may lead to nonphysical predictions. In the case of the power-law nonlinearity, if $\sigma d \geq 2$, initial data with mass (L^2 norm) in excess of the ground state may blow up in finite time (Sulem and Sulem 1999). However, experiments in the optical setting show that there is no "singularity" to speak of; the intensity of the solutions remains finite (Josserand and Rica 1997).

The model equation can be corrected to suppress singularity formation by replacing the power nonlinearity with a *saturated* nonlinearity. Ideally, such a nonlinearity allows potentially unstable behavior at low intensity but regularizes it at high intensity. One example of such a nonlinearity is the cubic-quintic, where $g(s) = s - \gamma s^2$. The cubic-quintic NLS (CQNLS) equation appears as a correction to the many body system that includes (repulsive) three body delta function interactions (Barashenkov et al. 1989; Barashenkov and Panova 1993). CQNLS also appears in models of super fluids, (Josserand et al. 1995), and in nonlinear optics, (Dimitrevski et al. 1998; Quiroga-Teixeiro and Michinel 1997; Wright et al. 1995).

Another saturated nonlinearity appearing in the optics literature is $g(s) = s/(1+s)$, (Tikhonenko et al. 1996). This nonlinearity was used in Eisner and Turkington (2006) to study turbulence for a one dimensional, nonintegrable equation without singularity formation. In laser plasma interactions, $g(s) = 1 - e^{-s}$ is used, (Johnston et al. 1997). In all cases, the Taylor expansion of the nonlinearity leads to CQNLS at second order.

In this work, we consider saturated nonlinearities of the form

$$g(s) = s^{\frac{q}{2}} \frac{s^{\frac{p-q}{2}}}{1 + s^{\frac{p-q}{2}}}, \tag{1.2}$$

where $2 + \frac{4}{d-2} > p > 2 + \frac{4}{d} > \frac{4}{d} > q > 0$ for $d \geq 3$ and $\infty > p > 2 + \frac{4}{d} > \frac{4}{d} > q > 0$ for $d < 3$. For $|u|$ large, (1.1) behaves as though it were L^2 subcritical while for

$|u|$ small, it behaves as though it were L^2 supercritical. Note that this choice of saturated nonlinearity is focusing for all values of $|u|$. For our purposes, p must be chosen substantially larger than the L^2 critical exponent, $\frac{4}{d}$, in order to allow sufficient regularity when linearizing the equation. For our numerical analysis, we work in one spatial dimension with the specific nonlinearity

$$g(s) = \frac{s^3}{1+s^2}. \tag{1.3}$$

A soliton solution of (1.1) is a function $u(t,x)$ of the form

$$u(t,x) = \mathrm{e}^{\mathrm{i}\omega t}\phi_\omega(x), \tag{1.4}$$

where $\omega > 0$ and $\phi_\omega(x)$ is a positive, spherically symmetric, exponentially decaying solution of the equation:

$$\Delta\phi_\omega - \omega\phi_\omega + g\big(\phi_\omega^2\big)\phi_\omega = 0. \tag{1.5}$$

For our particular nonlinearity, for any $\omega > 0$, there is a unique solitary wave solution $\phi_\omega(x)$ to (1.5); see Berestycki and Lion (1983) and McCleod (1993).

For large ω the solitons are stable, while for small ω they are unstable. A precise stability criterion identifying stable and unstable regions is provided in Grillakis et al. (1990) and Shatah and Strauss (1985), generalizing earlier work on stability in Weinstein (1985, 1986). This amounts to examining the relation $\omega \mapsto \|\phi_\omega\|_{L^2}^2$, defining a *soliton curve*. Where it is increasing as a function of ω, the solitons are stable; where this function is decreasing the solitons are unstable. In Fig. 1, we plot this curve for several common choices of $g(s)$.

As can be seen numerically in Fig. 1, our saturated nonlinearity spawns a soliton of minimal mass. Certain asymptotic methods can be used to describe the nature of the curve–multiscale methods can provide the asymptotics as $\omega \to 0$, while variational methods can give the asymptotics as $\omega \to \infty$. However, in this work, we forego an analytic description of the soliton curve and focus on the minimal mass soliton shown to exist in the numerical plot. The minimal mass soliton is a distinguished case amongst the already special family of soliton solutions. Though solitons to the left and right of this minimum can readily be classified as stable or unstable, the theory fails at extrema (Weinstein 1985, 1986). This motivates a careful examination of the dynamics of the minimal mass soliton under perturbation.

Comech and Pelinovsky (2003) demonstrated that the minimal mass soliton possesses a fundamentally *nonlinear* instability. They accomplished this by finding a small perturbation that forces the solution a fixed distance away from the minimal mass soliton in finite time. Their technique reduces the problem to studying an ODE modeling the perturbation for short times. They show that the 0 solution to the ODE is unstable by appropriate choice of initial data.

The purpose of this work is to numerically explore the following conjecture.

Conjecture 1.1 *Though the minimal mass soliton is unstable on short time scales, we conjecture that, on longer time scales, any solutions which is initially a small perturbation of the minimal mass soliton will either disperse or eventually relax toward a nearby stable soliton.*

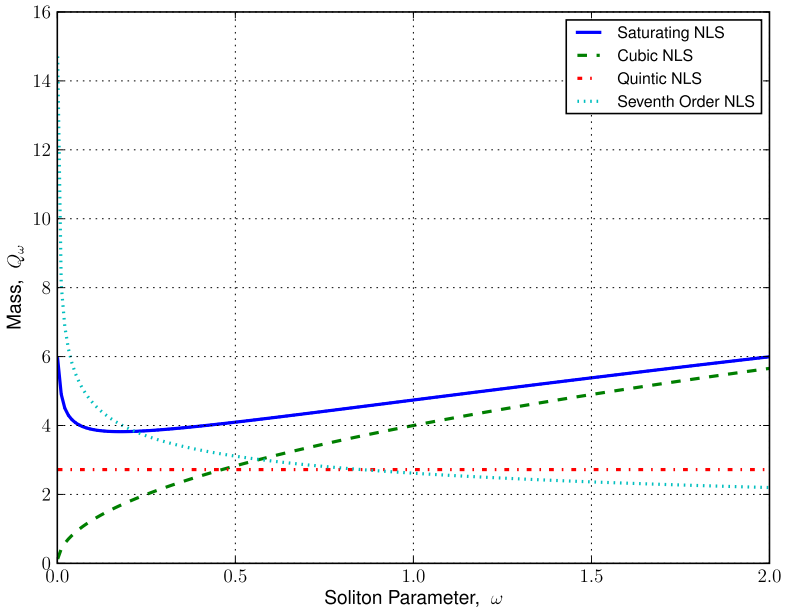

Fig. 1 Plots of the soliton curves ($\phi(\omega)$ with respect to ω) for a subcritical nonlinearity, critical nonlinearity, supercritical nonlinearity, and the saturated nonlinearity (1.3). The curves for the monomial nonlinearities are found analytically, while the curves for the saturated nonlinearities are found numerically using the method discussed in Sect. 4.1. All are in $d = 1$. Here, $\omega \geq 0.001$, as the supercritical and saturated cases diverge as $\omega \to 0$

This conjecture is part of the more general conjecture that any solution which does not disperse as $t \to \infty$ must eventually converge to a finite sum of stable solitons. Although the equation has a branch of unstable solitons, physically, it is expected that general solutions to (1.1) will resolve into stable solitons plus a dispersive component. This is referred to as the "soliton resolution" conjecture, a notoriously difficult problem to formulate. For nonlinearities with a specific two power structure, dynamics of this type were observed by Pelinovsky, Afanasjev, and Kivshar, who modeled the behavior of solutions near a minimal mass soliton by a second order ODE via adiabatic expansion in ω (Pelinovsky et al. 1996). This conjecture has also been explored numerically by Buslaev and Grikurov for two power nonlinearities in Buslaev and Grikurov (2001), where they found that a solution which is initially a perturbation of an unstable soliton tends to approach and then oscillate around a stable soliton.

By contrast, our method uses the full dynamical system of modulation parameters to find a 4-dimensional system of ODEs which is structured to allow for eventual recoupling to the continuous spectrum. Following Comech and Pelinovsky (2003), we begin with the ansatz that our solution is a small perturbation of the minimal mass soliton. We then break the perturbation into discrete and continuous spectral components relative to the linearization of the Schrödinger operator about the soliton. The discrete portion yields a 4-dimensional system of nonlinear ODEs. In this work, we neglect the continuous spectrum, although it may be included in a future work. We

further simplify the system by expanding the equations in powers of the dependent variables and dropping cubic and higher terms.

An obstacle in studying these ODEs is that the signs and magnitudes of the coefficients are not self-evident, necessitating numerical methods. We compute these values, which are intimately related to the minimal mass soliton, using the sinc spectral method. The use of the sinc function for numerically solving differential equations dates to Stenger (1979). It has been successfully used in a wide variety of linear and nonlinear, time dependent and independent, differential equations (Al-Khaled 2001; Bellomo and Ridolfi 1995; Bialecki 1991; Carlson et al. 1997; El-Gamel 2007; Lund and Bowers 1992; Revelli and Ridolfi 2003; Stenger 2000). In this work, we first numerically solve (1.5) for the soliton as a nonlinear collocation problem. We then use this information to compute the generalized kernel of the operator after linearization about the soliton.

With these coefficients in hand, we numerically integrate the ODE system, plotting the results. We find that there are two different types of behavior for the finite dimensional system, depending on the initial data. If the initial data represents a solution which our nonlinear PDE solver indicates can support a soliton, then we find that the solution is oscillatory. It is initially attracted to the stable side of the curve, and, over intermediate time scales, oscillates around a stable soliton close to the minimal mass soliton. If we initialize with the unstable conditions found in Comech and Pelinovsky (2003), the ODEs initially move in the unstable direction but quickly reverse, before commencing oscillation. On the other hand, if we begin with initial conditions which are expected to disperse as $t \to \infty$, the finite dimensional dynamics push the solution along the unstable soliton curve towards the value $\omega = 0$ rather quickly. This solution agrees with the numerically computed solution of the primitive equation (1.1) with corresponding initial data for as long as the mass conservation of the solution allows, after which our model continues to follow the unstable soliton curve but the actual solution disperses. In Pelinovsky et al. (1996), the authors observed similar dynamics, with both oscillatory and dispersive regimes.

These ODEs are an approximation valid on a short time interval. This study is the beginning of an analysis to show that perturbations of the minimal mass soliton are attracted to the stable side of the soliton curve. In a forthcoming work, we hope to show how the continuous-spectrum part of the perturbation interacts with the discrete-spectrum perturbation. Based on the work of Soffer and Weinstein (1999) we expect coupling to the continuous spectrum to cause radiation damping, which will ultimately cause the solution to have damped oscillations and select a soliton on the stable side of the curve.

This paper is organized as follows. In Sect. 2, we introduce preliminaries and necessary definitions. In Sect. 3, we derive the system of ODEs. In Sect. 4, we explain our numerical methods for finding the coefficients of the ODEs. In Sect. 5, we show the numerical solutions of the ODEs and explain our results. Finally, in Sect. 6, we present our conclusions and plans for future work. An Appendix contains details of our numerical method for computation of the soliton and related coefficients.

2 Definitions and Setup

Equation (1.1) is globally well-posed in H^1, the usual Sobolev space, with norm

$$\|u\|_{H^1}^2 = \|u\|_{L^2}^2 + \|\nabla u\|_{L^2}^2.$$

The global well-posedness for initial data in H^1 follows from the standard well-posedness theory for semilinear Schrödinger equations. Additionally, we assume that u_0 is spherically symmetric (which means even in one dimension), implying $u(x,t) = u(|x|,t)$ for all $t > 0$. Proofs can be found in numerous references including Cazenave (2003) and Sulem and Sulem (1999).

For data $u_0 \in H^1$, there are several conserved quantities. Particularly important invariants are:

Conservation of Mass (or Charge)

$$Q(u) = \frac{1}{2}\int_{\mathbb{R}^d} |u|^2 \,\mathrm{d}x = \frac{1}{2}\int_{\mathbb{R}^d} |u_0|^2 \,\mathrm{d}x.$$

Conservation of Energy

$$E(u) = \int_{\mathbb{R}^d} |\nabla u|^2 \,\mathrm{d}x - \int_{\mathbb{R}^d} G\big(|u|^2\big)\,\mathrm{d}x = \int_{\mathbb{R}^d} |\nabla u_0|^2 \,\mathrm{d}x - \int_{\mathbb{R}^d} G\big(|u_0|^2\big)\,\mathrm{d}x,$$

where

$$G(t) = \int_0^t g(s)\,\mathrm{d}s.$$

Detailed proofs of these conservation laws can be easily arrived at by using energy estimates or Noether's theorem, which relates conservation laws to symmetries of an equation. See Sulem and Sulem (1999) for details.

With this type of nonlinearity, it is known that soliton solutions to NLS exist and are unique. Existence of solitary waves for nonlinearities of the type (1.2) is proved in Berestycki and Lion (1983): in $\mathbb{R}^1$ via ODE techniques, and in higher dimensions by minimizing the functional

$$T(u) = \int |\nabla u|^2 \,\mathrm{d}x$$

with respect to the functional

$$V(u) = \int \left[G\big(|u|^2\big) - \frac{\omega}{2}|u|^2 \right] \mathrm{d}x.$$

Then, using a minimizing sequence and Schwarz symmetrization, one infers the existence of the nonnegative, spherically symmetric, decreasing soliton solution. Once we know that minimizers are radially symmetric, uniqueness can be established via a shooting method, showing that the desired soliton occurs at only one initial value, (McCleod 1993).

Of great importance is the fact that $Q_\omega := Q(\phi_\omega)$ and $E_\omega := E(\phi_\omega)$ are differentiable with respect to ω. This can be determined from the works of Shatah, namely (Shatah 1983, 1985). Differentiating (1.5), Q and E all with respect to ω, we have the relation

$$\partial_\omega E_\omega = -\omega \partial_\omega Q_\omega.$$

Numerical computations show that if we plot Q_ω with respect to ω for the saturated nonlinearity, the soliton curve goes to ∞ as ω goes to 0 or ∞ and has a global minimum at some $\omega = \omega_* > 0$; see Fig. 1.

We are interested in the stability of these explicit solutions under perturbations of the initial data. Recall the following notions of stability:

Definition 2.1 The soliton is said to be orbitally stable if, $\forall \epsilon > 0$, $\exists \delta > 0$ such that, for any initial data u_0 such that $\|u_0 - \phi_\omega\|_{H^1} < \delta$, for any $t < 0$, there is some $\theta \in \mathbb{R}$ such that $\|u(x,t) - e^{i\theta}\phi_\omega(x)\|_{H^1} < \epsilon$.

Definition 2.2 The soliton is said to be asymptotically stable, if $\exists \delta > 0$ such that if $\|u_0 - \phi_\omega\|_{H^1} < \delta$, then $\exists \tilde{\omega}, \tilde{\theta} > 0$ and $\psi_0 \in H^1$ such that $\|u(x,t) - \mathrm{e}^{\mathrm{i}\tilde{\omega}t+\tilde{\theta}}\phi_{\tilde{\omega}}(x) - \mathrm{e}^{\mathrm{i}t\Delta}\psi_0\|_{H^1} \to 0$ as $t \to \infty$.

Remark 2.1 Orbital stability suggests that a solution to (1.1) initially near the soliton will remain near the soliton in the H^1 norm. However, asymptotic stability states that the system actually selects a specific soliton to which it converges as time goes to ∞. Note, technically a system can undergo a very large change in ω and still be "asymptotically stable" provided it converges to a soliton for large time. However, asymptotic stability is usually proved using perturbation theory, which would suggest that in Definition 2.2, there would exist an $\epsilon > 0$ depending on δ such that

$$|\omega - \tilde{\omega}| < \epsilon.$$

Variational techniques developed in Weinstein (1985) and Weinstein (1986) and generalized to an abstract setting in Grillakis et al. (1990) and Shatah and Strauss (1985) tell us that when $\delta(\omega) = E_\omega + \omega Q_\omega$ is convex, or $\delta''(\omega) > 0$, we are guaranteed stability under small perturbations, while for $\delta''(\omega) < 0$ we are guaranteed that the soliton is unstable under small perturbations. For a brief reference on this subject, see Chap. 4 of Sulem and Sulem (1999). For nonlinearities that are twice differentiable at the origin and of monomial type at infinity (which would include our saturated nonlinearities), asymptotic stability has been studied for a finite collection of strongly orbitally stable solitons by Buslaev and Perelman (1995), Cuccagna (2003), and Rodnianski et al. (2003).

At a minimum of Q_ω, soliton instability is more subtle, because it is due solely to nonlinear effects. See Comech and Pelinovsky (2003), where this purely nonlinear instability is proved to occur by reducing the behavior of the discrete part of the spectrum to an ODE that is unstable for certain initial conditions.

2.1 Linearization about a Soliton

Throughout this section, we use vector notation, $\vec{\cdot}$, to represent complex functions. Any function written without vector notation is assumed to be real. For example, the complex valued scalar function $u + iv$ will be written $\binom{u}{v}$. In this notation, multiplication by i is represented by the matrix $J = \left(\begin{smallmatrix} 0 & -1 \\ 1 & 0 \end{smallmatrix}\right)$. We denote by $\vec{\phi}_\omega$ the complex vector $\binom{\phi_\omega}{0}$, where ϕ_ω is the real profile of the soliton with parameter ω. For simplicity, we suppress the ω subscript, writing ϕ in place of ϕ_ω.

For later reference, we now explicitly characterize the linearization of NLS about a soliton solution. First, consider the linear evolution of the perturbation of a soliton via the ansatz:

$$\vec{u} = \mathrm{e}^{J\omega t}\big(\vec{\phi}_\omega(x) + \vec{\rho}(x,t)\big) \tag{2.1}$$

with $\vec{\rho} = \binom{\rho_{\mathrm{Re}}}{\rho_{\mathrm{Im}}}$. For the purposes of finding the linearized Hamiltonian at ϕ_ω, we do not need to allow the parameters θ and ω to modulate, but when we develop our full system of equations in Sect. 3 parameter modulation will be taken into account. Inserting (2.1) as an ansatz into (1.1) we know that since ϕ is a soliton solution we have

$$J(\vec{\rho})_t + \Delta(\vec{\rho}) - \omega\vec{\rho} = -g\big(\phi^2\big)\vec{\rho} - 2g'\big(\phi^2\big)\phi^2\begin{pmatrix}\rho_{\mathrm{Re}}\\ 0\end{pmatrix} + O\big(|\vec{\rho}|^2\big). \tag{2.2}$$

(This calculation is explained in more detailed at the start of Sect. 3.) Here, we have used the following calculation of the nonlinear terms of the perturbation equation:

$$\begin{aligned}
&\big(g\big(|\phi+\rho|^2\big)(\phi+\rho) - g\big(|\phi|^2\big)\phi\big)\\
&\quad = \big(g\big(\phi^2 + 2\phi\rho_{\mathrm{Re}} + \rho_{\mathrm{Re}}^2 + \rho_{\mathrm{Im}}^2\big)(\phi + \rho_{\mathrm{Re}} + \mathrm{i}\rho_{\mathrm{Im}}) - g\big(\phi^2\big)\phi\big)\\
&\quad = g'\big(\phi^2\big)\big(\rho_{\mathrm{Re}}^2 + 2\phi\rho_{\mathrm{Re}} + \rho_{\mathrm{Im}}^2\big)(\phi + \rho_{\mathrm{Re}} + \mathrm{i}\rho_{\mathrm{Im}})\\
&\qquad + \frac{1}{2}g''\big(\phi^2\big)\big(\rho_{\mathrm{Re}}^2 + 2\phi\rho_{\mathrm{Re}} + \rho_{\mathrm{Im}}^2\big)^2(\phi + \rho_{\mathrm{Re}} + \mathrm{i}\rho_{\mathrm{Im}}) + \text{h.o.t.s.}
\end{aligned} \tag{2.3}$$

The linear terms will be absorbed into the linearized operator $J\mathcal{H}_\omega$, while the quadratic terms are handled explicitly; the $\mathcal{O}(\rho^2)$ terms in the expansion of the equation around ϕ_ω will be denoted by $N(\omega,\rho)$ in the sequel. In this work, after expansion in powers of ρ, we drop all terms of order greater than two.

We are interested in studying the linearized equation:

$$\partial_t\begin{pmatrix}\rho_{\mathrm{Re}}\\ \rho_{\mathrm{Im}}\end{pmatrix} = J\mathcal{H}\begin{pmatrix}\rho_{\mathrm{Re}}\\ \rho_{\mathrm{Im}}\end{pmatrix} + \text{h.o.t.}, \tag{2.4}$$

where

$$\mathcal{H} = \begin{pmatrix} 0 & L_- \\ -L_+ & 0\end{pmatrix}, \tag{2.5}$$

$$L_- = -\Delta + \omega - g(\phi_\omega), \tag{2.6}$$

$$L_+ = -\Delta + \omega - g(\phi_\omega) - 2g'\big(\phi_\omega^2\big)\phi_\omega^2. \tag{2.7}$$

Definition 2.3 A Hamiltonian, $\mathcal{H}$ is called admissible if the following hold:

(1) There are no embedded eigenvalues in the essential spectrum,
(2) The only real eigenvalue in $[-\omega, \omega]$ is 0,
(3) The values $\pm\omega$ are nonresonant.

Definition 2.4 Let NLS be taken with nonlinearity g. We call g admissible if there exists a minimal mass soliton, $\phi_{\min}$, for NLS and the Hamiltonian, $\mathcal{H}$, resulting from linearization about $\phi_{\min}$ is admissible in terms of Definition 2.3.

The spectral properties assumed for the linearized Hamiltonian equation in order to prove stability results are typically those from Definition 2.3; see (Buslaev and Perelman 1995; Demanet and Schlag 2006; Schlag 2009; Rodnianski et al. 2003; Krieger and Schlag 2006; Erdogan and Schlag 2006). However, we note that this condition is a constraint used to control the dispersive estimates necessary for perturbative analysis in analytic results, though it is sometimes possible to numerically solve this sort of problem even if Definition 2.3 does not hold; see, for example, Buslaev and Grikurov (2001).

In this work, we must simply assume that g is an admissible nonlinearity so that we may only concern ourselves with known discrete spectrum functions without coupling to endpoint resonances or embedded eigenvalues. However, this assumption is justified by the observed dynamics. Great care must be taken in studying the spectral properties of a linearized operator; although admissibility is expected to hold generically, certain algebraic conditions on the soliton structure itself factor into the analysis, often requiring careful numerical computations. See Demanet and Schlag (2006) as an introduction to such methods and the difficulties therein. To this end, in the forthcoming work (Marzuola and Simpson 2010), two of the authors look at analytic and computational methods for verifying these spectral conditions in the case of sufficiently supercritical monomial nonlinearities, though as of yet are unable to prove anything about saturated nonlinearities.

2.2 The Discrete Spectral Subspace

We approximate perturbations of the minimal mass soliton by projecting onto the discrete spectral subspace of the linearized operator. Notationally, we refer to P_d as the projection onto the finite dimensional discrete spectral subspace D_ω of H^1 relative to $\mathcal{H}$. Similarly, P_c represents projection onto the continuous spectral subspace for $\mathcal{H}$. We now describe, in detail, the discrete spectral subspace at the minimal mass.

Let ω^* be the value of the soliton parameter at which the minimal mass soliton occurs. It is proved in Comech and Pelinovsky (2003) (Lemma 3.8) that the discrete spectral subspace D_ω of $\mathcal{H}$ at ω^* has real dimension 4. This results from the extra orthogonality at minimal mass, which gives a dimension 4 generalized kernel exhibited by the following chain of equalities:

$$
\begin{aligned}
L_-\phi_{\omega^*} &= 0,\\
L_+(-\phi'_{\omega^*}) &= \phi_{\omega^*},\\
L_-\alpha &= -\phi'_{\omega^*},\\
L_+\beta &= \alpha.
\end{aligned}
$$

The functions $\vec{e}_1 = \binom{0}{\phi_\omega}$ and $\vec{e}_2 = \binom{\phi'_\omega}{0}$ are in the generalized kernel of $\mathcal{H}$ at every ω. Clearly, $\vec{e}_1$ is purely imaginary and $\vec{e}_2$ is real. In addition to $\vec{e}_1$ and $\vec{e}_2$, at ω^* there are two more linearly independent elements of D_ω, the purely imaginary $\vec{e}_3 = \binom{0}{\alpha}$ and the purely real $\vec{e}_4 = \binom{\beta}{0}$.

Applying Comech and Pelinovsky (2003) (Lemma 3.9), $\vec{e}_3$ and $\vec{e}_4$ can be extended as continuous functions of ω in such a way that $\vec{e}_3(\omega)$ is purely imaginary, $\vec{e}_4(\omega)$ is purely real. We write

$$
\vec{e}_3(\omega) = \begin{pmatrix} 0 \\ \alpha(\omega) \end{pmatrix}
$$

and

$$
\vec{e}_4(\omega) = \begin{pmatrix} \beta(\omega) \\ 0 \end{pmatrix},
$$

with α and β real-valued functions. The linearized operator, restricted to this subspace, is

$$
J\mathcal{H}(\omega)|_{D_\omega} = \begin{pmatrix} 0 & 1 & 0 & 0 \\ 0 & 0 & 1 & 0 \\ 0 & 0 & 0 & 1 \\ 0 & 0 & a(\omega) & 0 \end{pmatrix}, \tag{2.8}
$$

where $a(\omega)$ is a differentiable function that is equal to 0 at ω^*.

Before proceeding to the derivation of the ODEs, it is helpful to make a minor change of basis. Our goal is that, in the new basis, $\{\tilde{\vec{e}}_1, \tilde{\vec{e}}_2, \tilde{\vec{e}}_3, \tilde{\vec{e}}_4\}$, $\langle \tilde{\vec{e}}_1, \tilde{\vec{e}}_3 \rangle = 0$, which will make it easier for us to compute the dual basis. Replace $\vec{e}_3$ by

$$
\tilde{\vec{e}}_3 = \vec{e}_3 - \frac{\langle \vec{e}_1, \vec{e}_3 \rangle}{\|\vec{e}_1\|^2} \vec{e}_1 = \begin{bmatrix} 0 \\ \tilde{\alpha} \end{bmatrix}.
$$

To preserve the relationship $\vec{e}_3 = JH_\omega \vec{e}_4$, we need to replace $\vec{e}_4$ by

$$
\tilde{\vec{e}}_4 = \vec{e}_4 - \frac{\langle \vec{e}_1, \vec{e}_3 \rangle}{\|\vec{e}_1\|^2} \vec{e}_2 = \begin{bmatrix} \tilde{\beta} \\ 0 \end{bmatrix}.
$$

To preserve the relationship $JH_\omega \vec{e}_3 = \vec{e}_2 + a(\omega)\vec{e}_4$, we replace $\vec{e}_2$ by

$$
\tilde{\vec{e}}_2 = \left(1 + \frac{\langle \vec{e}_1, \vec{e}_3 \rangle}{\|\vec{e}_1\|^2}\right) \vec{e}_2 = \begin{bmatrix} \tilde{e_2} \\ 0 \end{bmatrix}.
$$

To preserve $JH_\omega \vec{e}_2 = \vec{e}_1$, we get that $\vec{e}_1$ must be replaced by

$$\tilde{\vec{e}}_1 = \left(1 + \frac{\langle \vec{e}_1, \vec{e}_3 \rangle}{\|\vec{e}_1\|^2}\right)\vec{e}_1 = \begin{bmatrix} 0 \\ \tilde{e_1} \end{bmatrix}.$$

With these substitutions, the JH_ω matrix on D_ω remains the same and we obtain the relationship $\langle \tilde{\vec{e}}_3, \tilde{\vec{e}}_1 \rangle = 0$. From here on, we will assume that we are working with this modified basis and simply take $\vec{e}_j := \tilde{\vec{e}}_j$ for $j = 1, 2, 3, 4$.

We will define $\vec{\xi}_i$ to be the dual basis to the revised $\vec{e}_i$ within D_ω. That is, the $\vec{\xi}_i$ are defined by $\vec{\xi}_i \in D_\omega$ and

$$\langle \vec{\xi}_i, \vec{e}_j \rangle = \delta_{ij}.$$

If we make the change of basis described above, then we can compute the $\vec{\xi}_j$ as follows. Define $D = \|\vec{e}_2\|^2 \|\vec{e}_4\|^2 - \langle \vec{e}_2, \vec{e}_4 \rangle^2$. Then:

$$\begin{aligned}
\vec{\xi}_1 &= \frac{1}{\|\vec{e}_1\|^2}\vec{e}_1, \\
\vec{\xi}_2 &= \frac{\|\vec{e}_4\|^2}{D}\vec{e}_2 - \frac{\langle \vec{e}_2, \vec{e}_4 \rangle}{D}\vec{e}_4, \\
\vec{\xi}_3 &= \frac{1}{\|\vec{e}_3\|^2}\vec{e}_3, \\
\vec{\xi}_4 &= -\frac{\langle \vec{e}_2, \vec{e}_4 \rangle}{D}\vec{e}_2 + \frac{\|\vec{e}_2\|^2}{D}\vec{e}_4.
\end{aligned}$$

As with the $\vec{e}_j$'s,

$$\vec{\xi}_j = \begin{bmatrix} 0 \\ \xi_j \end{bmatrix}$$

for $j = 1, 3$ and

$$\vec{\xi}_j = \begin{bmatrix} \xi_j \\ 0 \end{bmatrix}$$

for $j = 2, 4$ to distinguish between vectors and their scalar components.

3 Derivation of the ODEs

To derive the ODEs, we start with a small spherically symmetric perturbation of the minimal mass soliton, then project onto the discrete spectral subspace. Here, we closely follow Comech and Pelinovsky (2003).

We begin with the following ansatz, which allows θ and ω to modulate:

$$\vec{u}(t) = \mathrm{e}^{(\int_0^t \omega(t')\,\mathrm{d}t' + \theta(t))J}\left(\vec{\phi}_{\omega(t)} + \vec{\rho}(t)\right). \tag{3.1}$$

Here, we are suppressing the dependence of u, ϕ, and ρ on $|x|$ for notational simplicity. Recall we have assumed u to be spherically symmetric, so no other modulation

parameters occur. Unlike in Comech and Pelinovsky (2003) we do not assume that the rotation variable $\theta(t)$ is identically zero, so we need to include θ modulation in our full ansatz. Note that the derivation which follows applies for all nonlinearities in any dimension; specialization is required only to get explicit numerical results. This model includes the full dynamical system for spherically symmetric data and is designed in such a way that coupling to the continuous spectral subspace could easily be reintroduced. The authors plan to analyze the effect of that coupling, which is expected to be dissipative, in a future work.

Differentiating (3.1) with respect to t, we get

$$\vec{u}_t = \big[(\omega+\dot\theta)J(\vec\phi+\vec\rho)+\dot\omega\vec\phi'+\dot{\vec\rho}\big]\mathrm{e}^{\mathrm{i}(\int_0^t\omega(t')\,\mathrm{d}t'+\theta(t))},$$

where for a time dependent function $g(t)$ we represent differentiation with respect to t by $\partial_t g = \dot g$ and for an ω dependent function $f(\omega)$ we denote differentiation with respect to the soliton parameter ω by $\partial_\omega f = f'$. Plugging the above ansatz into (1.1) and canceling the phase term yields

$$-(\omega+\dot\theta)(\vec\phi+\rho)+\dot\omega J\vec\phi'+J\dot{\vec\rho}+\Delta\vec\phi+\Delta\vec\rho+g\big(|\phi+\rho|^2\big)(\vec\phi+\vec\rho)=0. \tag{3.2}$$

Recall that since ϕ is a soliton solution, $-\omega\phi+\Delta\phi+g(|\phi|^2)\phi=0$, yielding

$$-\dot\theta\vec\phi-(\omega+\dot\theta)(\vec\rho)+\dot\omega J\vec\phi'+J\dot{\vec\rho}+\Delta\vec\rho+g\big(|\vec\phi+\vec\rho|^2\big)(\vec\phi+\vec\rho)-g\big(\phi^2\big)\phi=0. \tag{3.3}$$

We multiply by J, solve for $\vec\rho$, and simplify. At the same time, we collect the $\Delta\vec\rho$ and $-\omega\vec\rho$ terms with the linear portion of $g(|\vec\phi+\vec\rho|^2)(\vec\phi+\vec\rho)-g(\phi^2)\vec\phi$, which yields JH_ω as defined in (2.5). The remaining terms of the nonlinearity are at least quadratic in ρ; recall that the quadratic terms are described in (2.3) and denoted $N(\omega,\rho)$.

Defining $\rho_j(t)$ as the coefficient of $\vec e_j(t)$ in ρ, we have

$$\vec\rho=\begin{bmatrix}\rho_{\mathrm{Re}}\\ \rho_{\mathrm{Im}}\end{bmatrix}=\rho_1\vec e_1+\rho_2\vec e_2+\rho_3\vec e_3+\rho_4\vec e_4+\vec\rho_c.$$

Then the above calculations give us

$$\dot{\vec\rho}=JH_\omega\vec\rho-\dot\theta\begin{pmatrix}0\\ \phi\end{pmatrix}-\dot\theta J\vec\rho-\dot\omega\begin{pmatrix}\phi'\\ 0\end{pmatrix}+\vec N(\omega,\vec\rho). \tag{3.4}$$

Taking the inner product of (3.4) with each of the $\vec\xi_i$ as defined in Sect. 2.2, and applying (2.8) yields the following system:

$$\begin{aligned}
\langle\vec\xi_1,\dot{\vec\rho}\rangle&=\rho_2-\dot\theta-\dot\theta\langle\vec\xi_1,J\vec\rho\rangle+\langle\vec\xi_1,\vec N\rangle,\\
\langle\vec\xi_2,\dot{\vec\rho}\rangle&=\rho_3-\dot\omega-\dot\theta\langle\vec\xi_2,J\vec\rho\rangle+\langle\vec\xi_2,\vec N\rangle,\\
\langle\vec\xi_3,\dot{\vec\rho}\rangle&=\rho_4-\dot\theta\langle\vec\xi_3,J\vec\rho\rangle+\langle\vec\xi_3,\vec N\rangle,\\
\langle\vec\xi_4,\dot{\vec\rho}\rangle&=a(\omega)\rho_3-\dot\theta\langle\vec\xi_4,J\vec\rho\rangle+\langle\vec\xi_4,\vec N\rangle.
\end{aligned} \tag{3.5}$$

From this point forward in our approximation, we drop the $\vec\rho_c$ component as a higher order error term. Using the product rule, we solve the left-hand side for $\dot\rho_i$ and put the

extra terms from the derivative of the operator that projects onto the discrete spectral subspace onto the right-hand side.

We have, as in Comech and Pelinovsky (2003), that

$$P_d\dot{\vec{\rho}} = \sum \vec{e}_j \dot{\rho}_j + \dot{\omega} \sum \vec{e}_i \Gamma_{ij} \rho_j - \dot{\omega} P_d P_d' \vec{\rho},$$

where we have implicitly defined

$$\Gamma_{ij} = \langle \xi_i, e_j' \rangle$$

and used that

$$P_d \frac{\mathrm{d}}{\mathrm{d}t} P_c \vec{\rho} = -\dot{\omega} P_d P_d' \vec{\rho}.$$

This gives

$$\begin{aligned}
\dot{\rho}_1 + \dot{\theta} &= \rho_2 - \dot{\theta}\langle \vec{\xi}_1, J\vec{\rho}\rangle + \langle \vec{\xi}_1, \vec{N}\rangle + \dot{\omega}\Big(\langle \vec{\xi}_1, P_d'\vec{\rho}\rangle - \sum \Gamma_{1j}\rho_j\Big),\\
\dot{\rho}_2 + \dot{\omega} &= \rho_3 - \dot{\theta}\langle \vec{\xi}_2, J\vec{\rho}\rangle + \langle \vec{\xi}_2, \vec{N}\rangle + \dot{\omega}\Big(\langle \vec{\xi}_2, P_d'\vec{\rho}\rangle - \sum \Gamma_{2j}\rho_j\Big),\\
\dot{\rho}_3 &= \rho_4 - \dot{\theta}\langle \vec{\xi}_3, J\vec{\rho}\rangle + \langle \vec{\xi}_3, \vec{N}\rangle + \dot{\omega}\Big(\langle \vec{\xi}_3, P_d'\vec{\rho}\rangle - \sum \Gamma_{3j}\rho_j\Big),\\
\dot{\rho}_4 &= a(\omega)\rho_3 - \dot{\theta}\langle \vec{\xi}_4, J\vec{\rho}\rangle + \langle \vec{\xi}_4, \vec{N}\rangle + \dot{\omega}\Big(\langle \vec{\xi}_4, P_d'\vec{\rho}\rangle - \sum \Gamma_{4j}\rho_j\Big).
\end{aligned} \tag{3.6}$$

There is also coupling to the continuous spectrum through terms such as $\langle \vec{\xi}_1, J\vec{\rho}\rangle$ which we omit. This can be included in the error term and is not analyzed in our finite dimensional system.

To make the system well determined, we must introduce two orthogonality conditions. The first is $\langle \rho, e_2\rangle = 0$, and the second is $\langle \rho, e_1\rangle = 0$. These represent the choice of $\omega(t)$ and $\theta(t)$ respectively that minimize the size of ρ, which yields $\rho_2 = \dot{\rho}_2 = 0$, and $\rho_1 = \dot{\rho}_1 = 0$, respectively.

The reduced system is then:

$$\begin{aligned}
\dot{\theta} &= -\dot{\theta}\langle \vec{\xi}_1, J\vec{\rho}\rangle + \langle \vec{\xi}_1, \vec{N}\rangle + \dot{\omega}\Big(\langle \vec{\xi}_1, P_d'\vec{\rho}\rangle - \sum \Gamma_{1j}\rho_j\Big),\\
\dot{\omega} &= \rho_3 - \dot{\theta}\langle \vec{\xi}_2, J\vec{\rho}\rangle + \langle \vec{\xi}_2, \vec{N}\rangle + \dot{\omega}\Big(\langle \vec{\xi}_2, P_d'\vec{\rho}\rangle - \sum \Gamma_{2j}\rho_j\Big),\\
\dot{\rho}_3 &= \rho_4 - \dot{\theta}\langle \vec{\xi}_3, J\vec{\rho}\rangle + \langle \vec{\xi}_3, \vec{N}\rangle + \dot{\omega}\Big(\langle \vec{\xi}_3, P_d'\vec{\rho}\rangle - \sum \Gamma_{3j}\rho_j\Big),\\
\dot{\rho}_4 &= a(\omega)\rho_3 - \dot{\theta}\langle \vec{\xi}_4, J\vec{\rho}\rangle + \langle \vec{\xi}_4, \vec{N}\rangle + \dot{\omega}\Big(\langle \vec{\xi}_4, P_d'\vec{\rho}\rangle - \sum \Gamma_{4j}\rho_j\Big).
\end{aligned} \tag{3.7}$$

In Comech and Pelinovsky (2003), the authors further reduce this system to prove there is an initial nonlinear instability. (Note that they have a slightly different system because they have assumed that $\theta \equiv 0$.) We are interested in the dynamics on an intermediate time scale; thus, we retain quadratically nonlinear terms in our equations.

Our notation is as follows. First, we have

$$\langle \vec{\xi}_1, J\vec{\rho}\rangle = \langle \xi_1, \rho_2\phi' + \rho_4\beta\rangle = \rho_4\langle \xi_1, \beta\rangle,$$

since $\rho_2 = 0$. Denote

$$c_{14} = \langle \xi_1(\omega^*), \beta(\omega^*)\rangle,$$

which is the lowest order term and the only one that will figure into our quadratic expansion. Notice that this is a real inner product of functions that normally do not appear in the same component of the complex vectors, because of the J in the equation.

Similarly, we have

$$\langle \vec{\xi}_2, J\vec{\rho}\rangle = \langle \xi_2, -\rho_1\phi - \rho_3\alpha\rangle = -\rho_3\langle \xi_2, \alpha\rangle,$$

since $\rho_1 = 0$. Denote

$$c_{23} = \langle \xi_2(\omega^*), \alpha(\omega^*)\rangle,$$

which is again the highest order term.

Then we have

$$\langle \vec{\xi}_3, J\vec{\rho}\rangle = \langle \xi_3, \rho_2\phi' + \rho_4\beta\rangle = \rho_4\langle \xi_3, \beta\rangle,$$

since $\rho_2 = 0$. Denote

$$c_{34} = \langle \xi_3(\omega^*), \beta(\omega^*)\rangle.$$

Finally, we have

$$\langle \vec{\xi}_4, J\vec{\rho}\rangle = \langle \xi_4, -\rho_1\phi - \rho_3\alpha\rangle = -\rho_3\langle \xi_4, \alpha\rangle,$$

since $\rho_1 = 0$. Denote by

$$c_{43} = \langle \xi_4(\omega^*), \alpha(\omega^*)\rangle.$$

We also write g_{ij} for the term $\Gamma_{ij}(\omega) = \langle \vec{\xi}_i, \vec{e}'_j\rangle$ at $\omega = \omega^*$.

Next, consider the terms $\langle \vec{\xi}_j, P'_d\vec{\rho}\rangle$. These terms are the e_j components of $P'_d\vec{\rho}$. We have

$$\begin{aligned}
P_d P'_d\vec{\rho} &= P_d\left[\sum_{j=1}^{4}\langle \vec{\xi}'_j, \vec{\rho}\rangle\vec{e}_j + \sum_{j=1}^{4}\langle \vec{\xi}_j, \vec{\rho}\rangle\vec{e}'_j\right] \\
&= \sum_{j=1}^{4}\sum_{k=3}^{4}\langle \vec{\xi}'_j, \vec{e}_k\rangle\rho_k\vec{e}_j + \rho_3 P_d\vec{e}'_3 + \rho_4 P_d\vec{e}'_4 \\
&= \sum_{j=1}^{4}\sum_{k=3}^{4}\langle \vec{\xi}'_j, \vec{e}_k\rangle\rho_k\vec{e}_j + \rho_3(\Gamma_{13}\vec{e}_1 + \Gamma_{33}\vec{e}_3) + \rho_4(\Gamma_{24}\vec{e}_2 + \Gamma_{44}\vec{e}_4) \\
&= \langle \vec{\xi}'_1, \vec{e}_3\rangle\rho_3\vec{e}_1 + \langle \vec{\xi}'_2, \vec{e}_4\rangle\rho_4\vec{e}_2 + \langle \vec{\xi}'_3, \vec{e}_3\rangle\rho_3\vec{e}_3
\end{aligned}$$

$$
\begin{aligned}
&+ \langle \vec{\xi}_4', \vec{e}_4 \rangle \rho_4 \vec{e}_4 \rho_3 (\Gamma_{13} \vec{e}_1 + \Gamma_{33} \vec{e}_3) + \rho_4 (\Gamma_{24} \vec{e}_2 + \Gamma_{44} \vec{e}_4) \\
&= \big(\langle \vec{\xi}_1', \vec{e}_3 \rangle + \Gamma_{13}\big) \rho_3 \vec{e}_1 + \big(\langle \vec{\xi}_2', \vec{e}_4 \rangle + \Gamma_{24}\big) \rho_4 \vec{e}_2 \\
&\quad + \big(\langle \vec{\xi}_3', \vec{e}_3 \rangle + \Gamma_{33}\big) \rho_3 \vec{e}_3 + \big(\langle \vec{\xi}_4', \vec{e}_4 \rangle + \Gamma_{44}\big) \rho_4 \vec{e}_4.
\end{aligned}
$$

Therefore, the relevant nonzero terms are

$$
\begin{aligned}
\langle \vec{\xi}_1, P_d' \vec{\rho} \rangle &= \big(\langle \vec{\xi}_1', \vec{e}_3 \rangle + \Gamma_{13}\big) \rho_3, \\
\langle \vec{\xi}_2, P_d' \vec{\rho} \rangle &= \big(\langle \vec{\xi}_2', \vec{e}_4 \rangle + \Gamma_{24}\big) \rho_4.
\end{aligned}
$$

We denote

$$
\begin{aligned}
p_{13} &= \big\langle \vec{\xi}_1'(\omega^*), \vec{e}_3(\omega^*) \big\rangle, \\
p_{33} &= \big\langle \vec{\xi}_3'(\omega^*), \vec{e}_3(\omega^*) \big\rangle,
\end{aligned}
$$

and

$$
\begin{aligned}
p_{24} &= \big\langle \vec{\xi}_2'(\omega^*), \vec{e}_4(\omega^*) \big\rangle, \\
p_{44} &= \big\langle \vec{\xi}_4'(\omega^*), \vec{e}_4(\omega^*) \big\rangle.
\end{aligned}
$$

Note that some cancellation will occur with the Γ_{ij} terms that appear separately in the system of ODEs, leaving only these p_{ij} terms in the finally system.

Finally, the terms $\langle \vec{\xi}_i, \vec{N}(\omega, \vec{\rho}) \rangle$ must be computed. We are only interested in the quadratic terms, which according to (2.3) are

$$
3Jg'\big(\phi^2\big)\phi\rho_{\mathrm{Re}}^2 + 2Jg''\big(\phi^2\big)\phi^2\rho_{\mathrm{Re}}^2 + Jg'\big(\phi^2\big)\phi\rho_{\mathrm{Im}}^2 + 2g'\big(\phi^2\big)\phi\rho_{\mathrm{Re}}\rho_{\mathrm{Im}}. \tag{3.8}
$$

Recall that, since ρ_1 and ρ_2 are 0, the projection onto the discrete-spectrum of ρ_{Re} is just $\rho_3 \vec{e}_3$ and the projection onto the discrete-spectrum of ρ_{Im} is just $\rho_4 \vec{e}_4$. We now have to compute the lowest-order terms of

$$
\big\langle \vec{\xi}_1, \vec{N}(\omega, \vec{\rho}) \big\rangle.
$$

The multiplier of ρ_3^2 in $\langle \vec{\xi}_1, \vec{N}(\omega, \vec{\rho}) \rangle$ is

$$
n_{133} = \big\langle \xi_1, \big(3g'\big(\phi^2\big)\phi + 2g''\big(\phi^2\big)\phi^2\big)e_3^2 \big\rangle.
$$

Similarly, we define

$$
\begin{aligned}
n_{144} &= \big\langle \xi_1, g'\big(\phi^2\big)\phi e_4^2 \big\rangle, \\
n_{234} &= \big\langle \xi_2, -2g'\big(\phi^2\big)\phi e_3 e_4 \big\rangle, \\
n_{333} &= \big\langle \xi_3, \big(3g'\big(\phi^2\big)\phi + 2g''\big(\phi^2\big)\phi^2\big)e_3^2 \big\rangle, \\
n_{344} &= \big\langle \xi_3, g'\big(\phi^2\big)\phi e_4^2 \big\rangle, \\
n_{434} &= \big\langle \xi_4, -2g'\big(\phi^2\big)\phi e_3 e_4 \big\rangle.
\end{aligned}
$$

Notice that, as in the computation of the c_{ij}, these are real inner products between real functions that normally appear in different components of the complex vectors.

Lastly, we need to estimate $a(\omega)$. Recall that $a(\omega^*) = 0$, and that $a(\omega)$ appears in (3.7) multiplied by ρ_3, so we are seeking only the linear term, $a(\omega) \sim a_0(\omega - \omega^*)$. We calculate, as in Lemma 3.10 of Comech and Pelinovsky (2003),

$$a_0 = a'(\omega^*) = -\frac{2}{\langle \phi_{\omega^*}, \beta \rangle} \big(\langle \phi'_{\omega^*}, \phi'_{\omega^*} \rangle - \langle \phi_{\omega^*}, \phi''_{\omega^*} \rangle \big).$$

With these assumptions, we conclude the following.

Proposition 3.1 *The quadratic approximation for the evolution of a perturbation of the minimal mass soliton,* (3.3)*, ignoring coupling to the continuous spectrum, is*

$$\begin{aligned}
\dot\theta &= -c_{14}\dot\theta\rho_4 + n_{133}\rho_3^2 + n_{144}\rho_4^2 + \dot\omega p_{13}\rho_3,\\
\dot\omega &= \rho_3 + c_{23}\dot\theta\rho_3 + n_{234}\rho_3\rho_4 + \dot\omega p_{24}\rho_4,\\
\dot\rho_3 &= \rho_4 - c_{34}\dot\theta\rho_4 + n_{333}\rho_3^2 + n_{344}\rho_4^2 + \dot\omega p_{33}\rho_3,\\
\dot\rho_4 &= a_0(\omega - \omega^*)\rho_3 + c_{43}\dot\theta\rho_3 + n_{434}\rho_3\rho_4 + \dot\omega p_{44}\rho_4.
\end{aligned} \tag{3.9}$$

In this system, we implicitly assume that θ, $(\omega - \omega^*)$, ρ_i and their time derivatives are all of the same order.

4 Numerical Methods

From here on, we use numerical techniques to analyze solutions to (3.9). We will work in one space dimension, with the specific saturated nonlinearity $g(s) = \frac{s^3}{1+s^2}$ as described in the Introduction. In this setting, our assumption of spherical symmetry on the initial data becomes an assumption that u_0 is even. Though we have a complete description of the generalized kernel of $J\mathcal{H}$, including its size and the relation among the elements, nothing is expressible in terms of elementary functions. As this kernel determines the coefficients in our ODE system, we numerically compute it, permitting us to subsequently integrate the ODEs numerically.

The sinc function, $\sin(\pi x)/(\pi x)$ was used to compute solitary wave solutions when analytical expressions were not readily available in Lundin (1980). It has also been used to study time dependent nonlinear wave equations (Al-Khaled 2001; Revelli and Ridolfi 2003; Bellomo and Ridolfi 1995; Carlson et al. 1997), and a variety of linear and nonlinear boundary value problems (Bialecki 1989, 1991; El-Gamel et al. 2003; El-Gamel and Zayed 2004; El-Gamel 2007; Mohsen and El-Gamel 2008).

We will use the sinc function to estimate the coefficients in three steps:

- Compute a discrete representation of the minimal mass soliton, ϕ_{ω^*}.
- Compute discrete representations of the generalized kernel of $\mathcal{H}$, i.e., the derivatives with respect to ω.
- Compute necessary inner products for the coefficients.

4.1 Sinc Discretization

The problem of finding a soliton solution of (1.5) is a nonlinear boundary value problem posed on $\mathbb{R}$. We respect this description in our discretization by approximating functions with the sinc spectral method. This technique is thoroughly explained in (Lund and Bowers 1992; Stenger 1993, 1981, 2000) and briefly in Appendix A.1. In the sinc discretization, the problem remains posed on $\mathbb{R}$ and the boundary conditions, that the solution vanish at $\pm\infty$, are naturally incorporated.

Given a function $u(x)\colon \mathbb{R} \to \mathbb{R}$, u is approximated using a superposition of shifted and scaled sinc functions:

$$C_{M,N}(u,h)(x) \equiv \sum_{k=-M}^{N} u_k \operatorname{sinc}\left(\frac{x-x_k}{h}\right) = \sum_{k=-M}^{N} u_k S(k,h)(x), \tag{4.1}$$

where $x_k = kh$ for $k = -M, \ldots, N$ are the *nodes* and $h > 0$. There are *three* parameters in this discretization, h, M, and N, determining the number of and spacing of lattice points. This is common to numerical methods posed on unbounded domains; see Boyd (2001).

A useful and important feature of this spectral method is that, when evaluated at a node,

$$C_{M,N}(u,h)(x_k) = u_k. \tag{4.2}$$

Additionally, the convergence is rapid both in practice and theoretically. See Theorem A.1 in Appendix A.1 for a statement on optimal convergence.

Since the soliton is an even function, we may take $N = M$. We will thus write

$$C_M(u,h)(x) \equiv C_{M,M}(u,h)(x). \tag{4.3}$$

The symmetry implies $u_{-k} = u_k$ for $k = -M, \ldots, M$. We take advantage of this constraint in our computations. In addition, we slave h to M in accordance with (A.8).

To compute a discrete sinc approximation of the ground state, we frame the soliton equation as a *nonlinear collocation problem.* Approximating $\phi(x)$ as in (4.1), we seek coefficients $\{R_k\}$ such that

$$\begin{aligned} &\partial_x^2 C_M(\phi,h)(x_k) - \lambda C_M(\phi,h)(x_k) + g\big(\big|C_M(\phi,h)(x_k)\big|^2\big) C_M(\phi,h)(x_k) = 0, \\ &\quad \text{for } k = -M, \ldots, M. \end{aligned} \tag{4.4}$$

By satisfying (4.4), the discrete approximation solves the soliton equation in the *strong* sense at the nodes, also known as *collocation points*. This is in contrast to a Galerkin formulation, which solves the equation in the weak sense. However, for the one-dimensional problem under consideration, sinc-Galerkin and sinc-collocation lead to the same algebraic system.

Equation (4.4) yields a system of nonlinear algebraic equations. Let $\vec{\phi}$ be the column vector associated with the discrete approximation of ϕ:

$$C_M(\phi,h)(x_k)\mapsto\vec{\phi}=\begin{pmatrix}\phi_{-M}\\ \phi_{-M+1}\\ \vdots\\ \phi_M\end{pmatrix}. \tag{4.5}$$

Differentiation of a sinc approximated function that is evaluated at the collocation points corresponds to matrix multiplication:

$$\partial_x^2 C_M(\phi,h)(x_k)\mapsto D^{(2)}\vec{\phi}. \tag{4.6}$$

Explicitly, $D^{(2)}$ is

$$D^{(2)}_{jk}=\frac{\mathrm{d}^2}{\mathrm{d}x^2}S(j,h)(x)|_{x=x_k}=\begin{cases}\frac{1}{h^2}\frac{-\pi^2}{3}, & j=k,\\ \frac{1}{h^2}\frac{-2(-1)^{k-j}}{(k-j)^2}, & j\neq k.\end{cases} \tag{4.7}$$

Using (4.2),

$$g\big(\big|C_M(\phi,h)(x_k)\big|^2\big)C_M(\phi,h)(x_k)=C_M\big(g\big(|\phi|^2\big)\phi,h\big)(x_k)=g\big(|\phi_k|\big)^2\phi_k.$$

Thus,

$$g\big(\big|C_M(\phi,h)(x_k)\big|^2\big)C_M(\phi,h)(x_k)\mapsto g\big(|\vec{\phi}|^2\big)\vec{\phi}\equiv\begin{pmatrix}g(|\phi_{-M}|^2)\phi_{-M}\\ \vdots\\ g(|\phi_M|^2)\phi_M\end{pmatrix}.$$

With these relations, the discrete system is

$$D^{(2)}\vec{\phi}-\omega\vec{\phi}+g\big(|\vec{\phi}|^2\big)\vec{\phi}=0. \tag{4.8}$$

It is this equation to which we apply a nonlinear solver, subject to an appropriate guess. We discuss an important subtlety in Appendix A.2.

4.2 Computing the Minimal Mass

Now that we have an algorithm for finding a discrete representation of a soliton, we seek to find the value of the soliton parameter for the one possessing minimal mass, along with the corresponding discretized soliton. The sinc discretization has the property that the $L^2(\mathbb{R})$ inner product is well approximated by

$$\langle f,g\rangle=\int fg\,\mathrm{d}x\approx\sum_{-M}^{M}hf_kg_k=h(\vec{f}\cdot\vec{g}).$$

Thus, the mass of the soliton can be estimated by

$$\|\phi\|_{L^2}^2 \approx h|\vec{\phi}|^2.$$

Recognizing that $\vec{\phi} = \vec{\phi}(\omega)$, we seek to minimize the functional $h|\vec{\phi}(\omega)|^2$ with respect to ω. The argument ω for which the minimum occurs will be ω^*. To find the minimal mass, we take the derivative, getting a discrete representation of the minimal mass orthogonality condition:

$$2h\vec{\phi} \cdot \vec{\phi}' = 0. \tag{4.9}$$

We solve (4.9) to find ω^*, computing $\vec{\phi_{\omega^*}}$ in the process.

The value of ω^* can be obtained by other algorithms. In the one-dimensional case, the soliton equation possesses a first integral, permitting the minimal mass to be computed by numerical quadrature and minimization; a comparison of our results and this approach appears in Appendix A.4.1. Though these approaches are quite accurate for the task of computing the minimal mass, they are inadequate at computing the generalized kernel. Thus, we seek to solve the problem consistently by finding the minimal mass for a given $2M + 1$ dimensional approximation of the problem.

4.3 Discretized Generalized Kernel

As seen in Sect. 2.2, at the minimal mass soliton ϕ_{ω^*}, there are four functions associated with the kernel satisfying the second order equations:

$$L_- \phi_{\omega^*} = 0, \tag{4.10}$$

$$L_+(-\phi'_{\omega^*}) = \phi_{\omega^*}, \tag{4.11}$$

$$L_- \alpha = -\phi'_{\omega^*}, \tag{4.12}$$

$$L_+ \beta = \alpha. \tag{4.13}$$

These four functions can also be discretized with sinc, as in (4.1). The operators, $L_\pm$, have discrete spectral representations:

$$L_+ \mapsto \mathbf{L}_+ \equiv -D^{(2)} + \omega I - \operatorname{diag}\{g(\vec{\phi}^2_{\omega^*})\}, \tag{4.14}$$

$$L_- \mapsto \mathbf{L}_- \equiv -D^{(2)} + \omega I - \operatorname{diag}\{g(\vec{\phi}^2_{\omega^*}) - 2g'(\vec{\phi}^2_{\omega^*})\vec{\phi}^2_{\omega^*}\}. \tag{4.15}$$

Taking $\vec{u} = \vec{\phi}$, we successively solve for $\vec{\phi}'$, $\vec{\alpha}$, and $\vec{\beta}$. A singular value decomposition must be used to get $\vec{\alpha}$ since $\mathbf{L}_-$ has a nontrivial kernel.

Furthermore, we compute discrete approximations of the derivatives of ϕ, ϕ', α, and β taken with respect to ω at ω^*. The relevant operators are formed analogously to (4.14) and (4.15).

4.4 Convergence

Amongst the many calculations made, the most important is of ω^*, the parameter of the minimal mass soliton. We summarize the results in Table 1. We see that $h|\vec{\phi}|^2$

Table 1 The convergence of the sinc discretization to the minimal mass soliton

M	$h\lvert\vec{\phi}\rvert^2$	ω^*
20	3.820771417633398	0.177000229690401
40	3.821145471868853	0.177576993694258
60	3.821148930202135	0.177587655985074
80	3.821149018422933	0.177588043323139
100	3.821149022493814	0.177588063805561
200	3.821149022780618	0.177588065432740
300	3.821149022780439	0.177588065432795
400	3.821149022780896	0.177588065433095
500	3.821149022780275	0.177588065432928

robustly converges, achieving twelve digits of precision and ω^* appears to achieve eleven digits of precision. These are consistent with the values in Table 4 from Appendix A.4, where they were computed using different methods.

For the purposes of our simulations, we believe we have sufficient precision, approximately ten significant digits, for the time integration of our system of ODEs. Some data for the convergence of the coefficients appearing in (3.9) is given in Appendix A.3.

5 Numerical Results

We explore here the dynamics of the finite dimensional system (3.9) and compare with solutions for the full nonlinear PDE (1.1) with corresponding initial data.

To solve (3.9), we use the solver `ode45` from MATLAB after properly preparing the initial data using the soliton-finding codes in Sect. 4.1.

5.1 PDE Solver

In order to determine the accuracy of our results, we also use a nonlinear solver to approximate the solutions with a perturbed minimal-mass soliton as initial data. For this nonlinear solver, we use a finite element scheme in space and a Crank–Nicholson scheme in time. This is similar to the method used in Holmer et al. (2007). In brief, we discretize our (1.1) by method of lines, using finite elements in space and Crank–Nicholson for time-stepping. This method is L^2 conservative, though it is not energy conserving. A similar scheme was implemented without potential in Akrivis et al. (2003), where the blow-up for NLS in several dimensions was investigated.

We require the spatial grid to be large enough to ensure negligible interaction with the boundary. As absorbing boundary conditions for cubic NLS currently require high frequency limits to apply successfully, we choose simply to carefully ensure that our grid is large enough in order for the interactions to be negligible throughout the experiment. For the convergence of such methods without potentials, see the references in Akrivis et al. (1991, 1997, 2003).

We select a symmetric region about the origin, $[-R, R]$, upon which we place a mesh of N elements. The standard hat function basis is used in the Galerkin approximation. We allow for a finer grid in a neighborhood of length 1 centered at the origin to better study the effects of the soliton interactions.

In terms of the hat basis, the PDE (1.1) becomes:

$$\langle u_t, v\rangle + \mathrm{i}\langle u_x, v_x\rangle/2 - \mathrm{i}\big\langle g\big(|u|^2\big)u, v\big\rangle = 0,$$
$$u(0,x) = u_0, \qquad u(t,x) = \sum_v c_v(t)v,$$

where $\langle\cdot,\cdot\rangle$ is the standard L^2 inner product, v is a basis function, and u, u_0 are linear combinations of the v's.

Since the v's are hat functions, we have a tridiagonal linear system. Let $h_t > 0$ be a uniform time step, and let

$$u_n = \sum_v c_v(nh_t)v$$

be the approximate solution at the nth time step. Implementing Crank–Nicholson, the system becomes:

$$\langle u_{n+1} - u_n, v\rangle + \mathrm{i}h_t\big\langle\big((u_{n+1}+u_n)/2\big)_x, v_x\big\rangle$$
$$= \mathrm{i}h_t\big\langle g\big(\big|\big(u_{n+1}+u_n\big)/2\big|^2\big)(u_{n+1}+u_n)/2, v\big\rangle, \qquad u_0 = \sum_v \alpha_v v.$$

By defining

$$y_n = (u_{n+1}+u_n)/2,$$

we have simplified our system to

$$\langle y_n, v\rangle + \mathrm{i}\frac{h_t}{4}\langle (y_n)_x, v_x\rangle = \mathrm{i}\frac{h_t}{2}\langle |y_n|^2 y_n, v\rangle + \langle u_n, v\rangle.$$

An iteration method from Akrivis et al. (2003) is now used to solve this nonlinear system of equations. Namely, we set

$$\big\langle y_n^{k+1}, v\big\rangle + \mathrm{i}\frac{h_t}{4}\big\langle \big(y_n^{k+1}\big)_x, v_x\big\rangle = \mathrm{i}\frac{h_t}{2}\big\langle \big|y_n^k\big|^2 y_n^k, v\big\rangle + \langle u_n, v\rangle.$$

We take $y_n^0 = u_n$ and perform three iterations in order to obtain an approximate solution.

For our problem, we have taken (1.1) with the nonlinearity

$$\frac{|u|^6}{1+|u|^4}u.$$

Then, the minimal mass soliton occurs at

$$\omega^* = 0.177588065433.$$

5.2 Results

With the numerical schemes outlined above, we then compare our finite dimensional model to the numerically integrated solution with appropriate initial data $\omega_0 = \omega(0) < \omega^*$, $\alpha_0 = \rho_3(0)$, $\beta_0 = \rho_4(0)$, and $\theta_0 = \theta(0) = 0$ for simplicity. In Figs. 3, 4, 5, we take $\beta_0 > 0$ and vary α_0, ω_0. Similarly, in Figs. 6, 7, 8, we take $\beta_0 < 0$ and once again vary α_0, ω_0. Note that we are comparing solutions to the ODEs to solutions of (1.1) with the correct initial parameters so that the initial profiles are identical. The initial data for both the finite and infinite dimensional solvers always consists of an orbitally unstable soliton being perturbed by elements of the generalized kernel of the linearized operator $\mathcal{H}$ at ω^*. Also, all the numerics we present are given in terms of plotting $|u(t, 0)|$, the amplitude of the solution at 0, versus time t. The computed correlation between the amplitude of a soliton ϕ_ω at 0 and the soliton parameter ω can be seen in Fig. 2.

When $\beta_0 > 0$, the initial data is expected to allow the admission of a solution with a soliton component as t increases. The finite dimensional system shows that if we initially perturb the system either toward the stable or the unstable side of the curve, the system produces immediate oscillations. Specifically, if the dynamics begin to diverge, the higher order nonlinear corrections in (3.9) arrest the solution, resulting in fairly uniform oscillations about the minimal mass soliton; see Figs. 3, 4, 5. As one can see, for initial values $\omega_0 \approx \omega^*$, we see a good fit for several oscillations of our finite dimensional approximation to the dynamics of the full solution. As expected, this weakens as ω_0 diverges from ω^* due to the nature of our approximations in

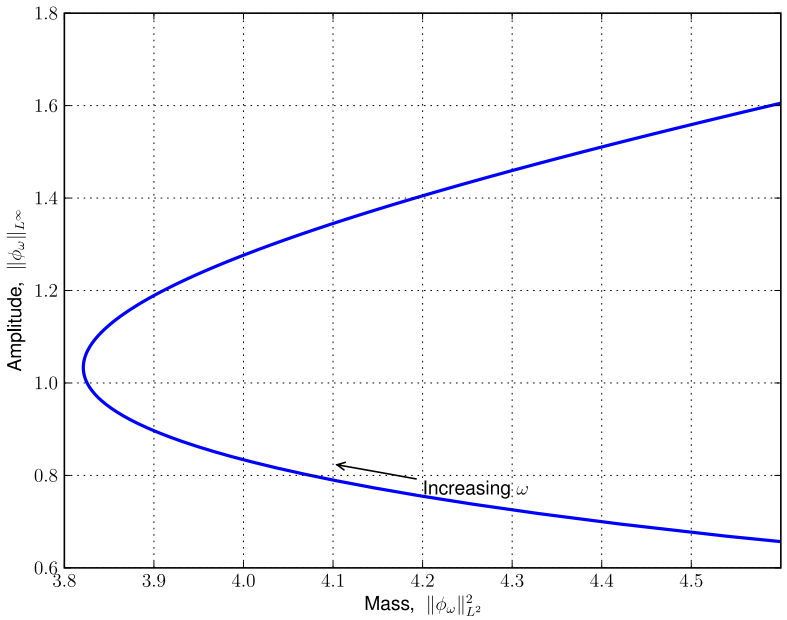

Fig. 2 A plot of the maximum amplitude with respect to the L^2 norm for a saturated nonlinear Schrödinger equation. Computed at $M + 1 = 101$ collocation points for $\omega \in [0.01, 1.5]$

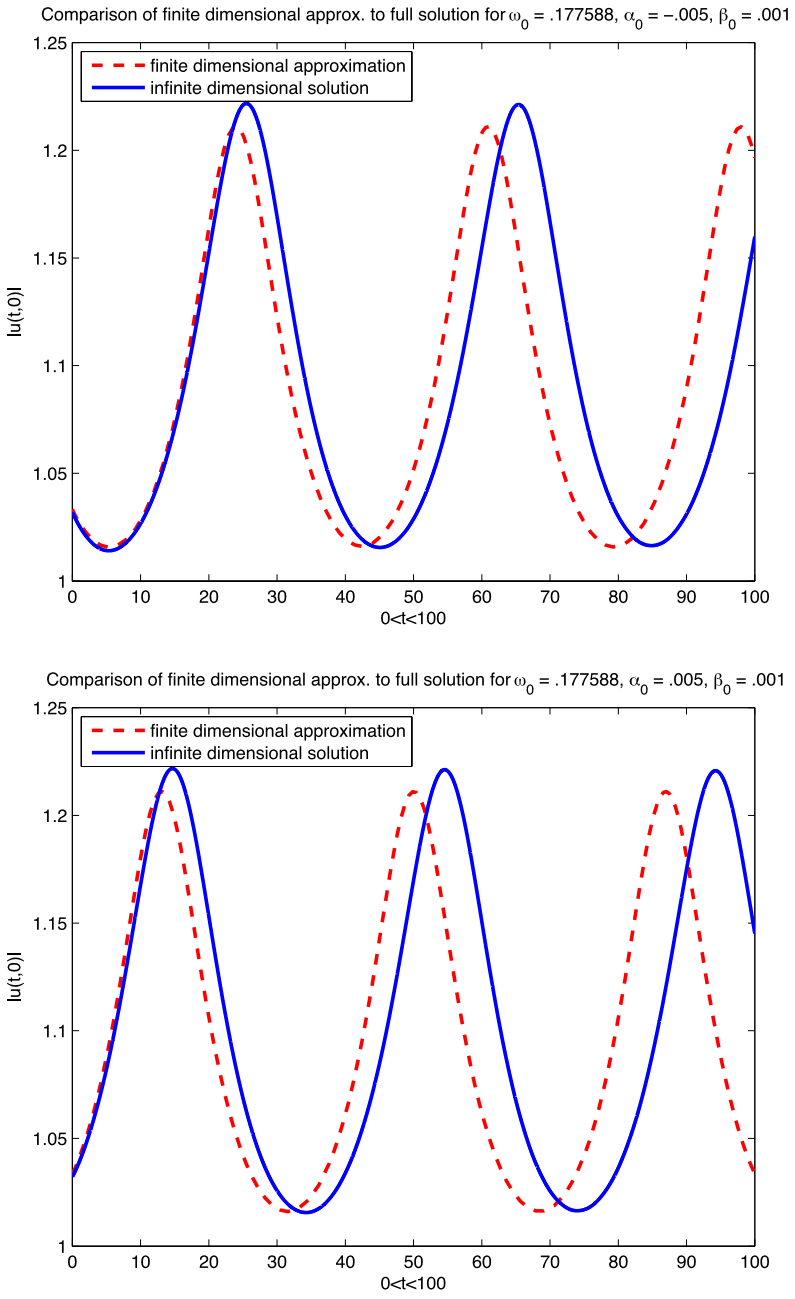

Fig. 3 A plot of the solution to the system of ODE's as well as the full solution to (1.1) derived for solutions near the minimal soliton for $\rho_3(0) > 0$ and $\rho_3(0) < 0$, $\rho_4(0) > 0$ for $\omega_0 = 0.177588$, $N = 1000$

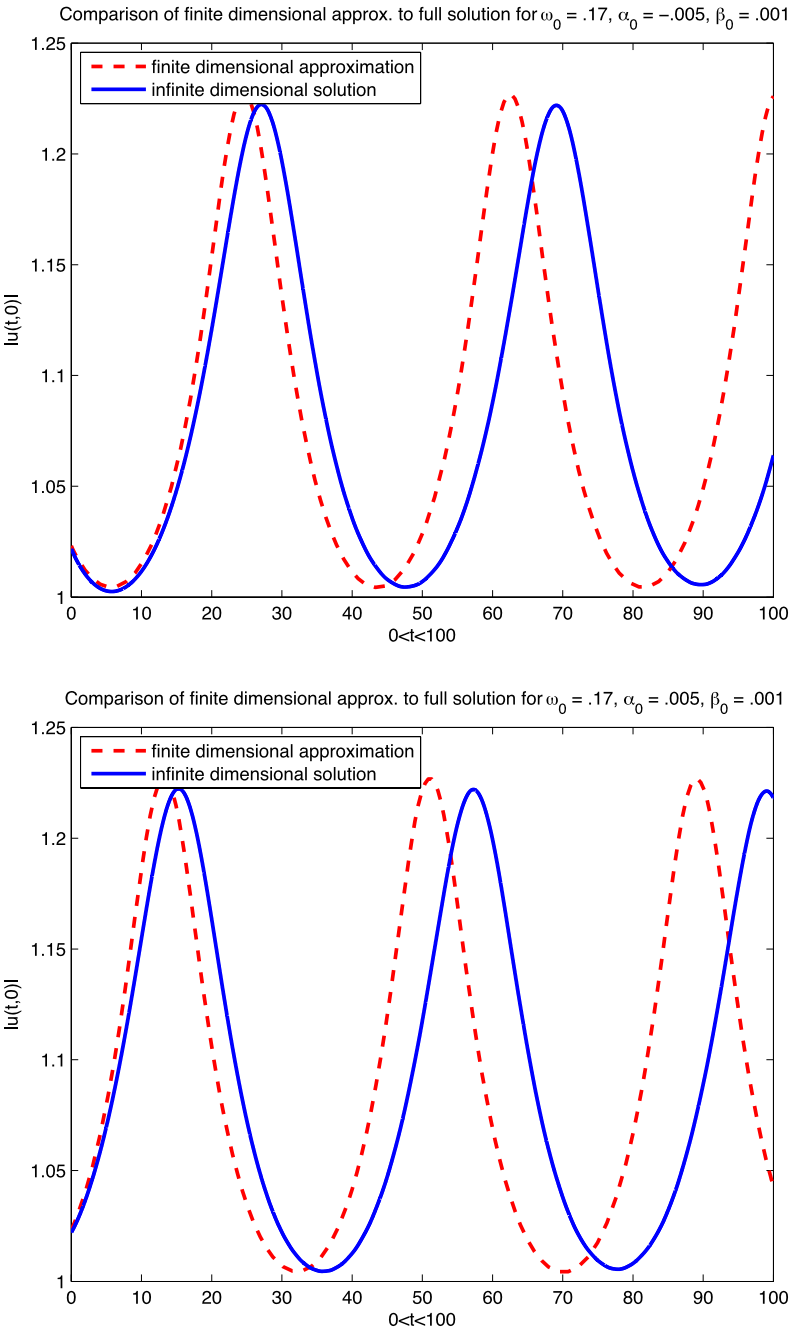

Fig. 4 A plot of the solution to the system of ODE's as well as the full solution to (1.1) derived for solutions near the minimal soliton for $\rho_3(0) > 0$ and $\rho_3(0) < 0$, $\rho_4(0) > 0$ for $\omega_0 = 0.17$, $N = 500$

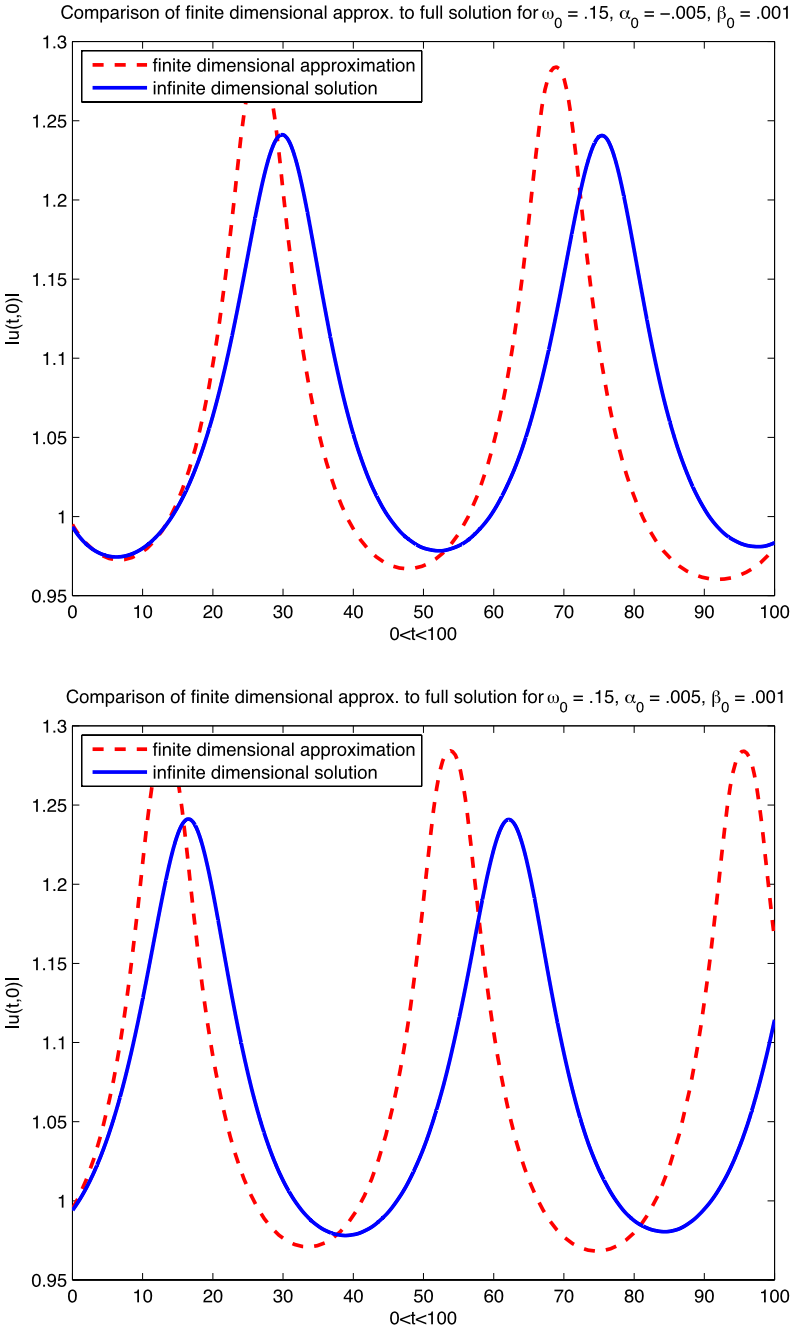

Fig. 5 A plot of the solution to the system of ODE's as well as the full solution to (1.1) derived for solutions near the minimal soliton for $\alpha_0 = \rho_3(0) > 0$ and $\alpha_0 = \rho_3(0) < 0$, $\beta_0 = \rho_4(0) > 0$ for $\omega_0 = 0.15$, $N = 500$

Sect. 3. We conjecture that such oscillations about the minimal mass when coupled to the continuous spectrum will lead generically to a damped convergence of the solution towards a stable soliton near the minimal mass soliton on a long time scale, similar to the oscillations observed in LeMesurier et al. (1988).

For $\beta_0 < 0$, and other initial parameters sufficiently small, the initial data is below the minimal mass and is expected to disperse as $t \to \infty$. In this regime, we see the amplitude fall below the value associated with the minimal mass soliton, forcing $\omega(t) < \omega_*$, the minimal mass value. Thus, we are on the unstable branch of the soliton curve. Clearly, conservation of mass for (1.1) forbids the primitive system from indefinitely behaving as a perturbed soliton with a progressively smaller value of ω. Indeed, we see divergence of the nonlinear solution from our solution as t increases. As our approximation is based on an expansion about ω_*, the deviation eventually renders it invalid.

However, on shorter time scales, there is reasonable agreement between the full solution and our finite dimensional approximation; see Figs. 6, 7, 8. This occurs regardless of whether we initially perturb in the stable or unstable direction. Our findings confirm the regimes predicted in Pelinovsky et al. (1996).

It remains to briefly comment on the convergence of our numerical methods. The ODE solver, `ode45`, for the finite dimensional system of ODEs is a standard Runge–Kutta method with known strong convergence results documented in a number of introductory texts on numerical methods. In addition, the finite element solver for the full nonlinear problem has well-established analytic convergence results; see Akrivis et al. (1991). Hence, the solutions for the corresponding systems are known to be accurate representations of the actual continuous solutions. Though we have not fully justified in this work the spectral decomposition used to derive (3.9), the fact that the infinite dimensional dynamics are so well approximated by the finite dimensional system constructed from these spectral assumptions is quite good evidence that this approximation is a valid one. However, as mentioned in Sect. 2.1, investigating the validity of spectral assumptions will be an important topic of future research.

6 Conclusions and Discussion of Future Work

In this work, we have used a sinc discretization method to compute the coefficients of the dynamical system (3.9), which is valid near the minimal mass soliton for a saturated nonlinear Schrödinger equation. We find that the dynamical system is an accurate approximation to the full nonlinear solution in a neighborhood of the minimal mass. Moreover, we see that there are two distinct regimes of the dynamical system.

The first regime given by $\rho_4(0) > 0$ represents oscillation along the soliton curve. The finite dimensional oscillations are valid solutions on long time scales in the conservative PDE, hence we may observe long time closeness of our finite dimensional approximation to the full solution of (1.1).

The second regime given by $\rho_4(0) < 0$ is the dispersive regime, which results in motion along the unstable branch of the soliton curve. Indeed, a perturbation of this type reduces the mass, which near the minimal mass should lead to dispersion in

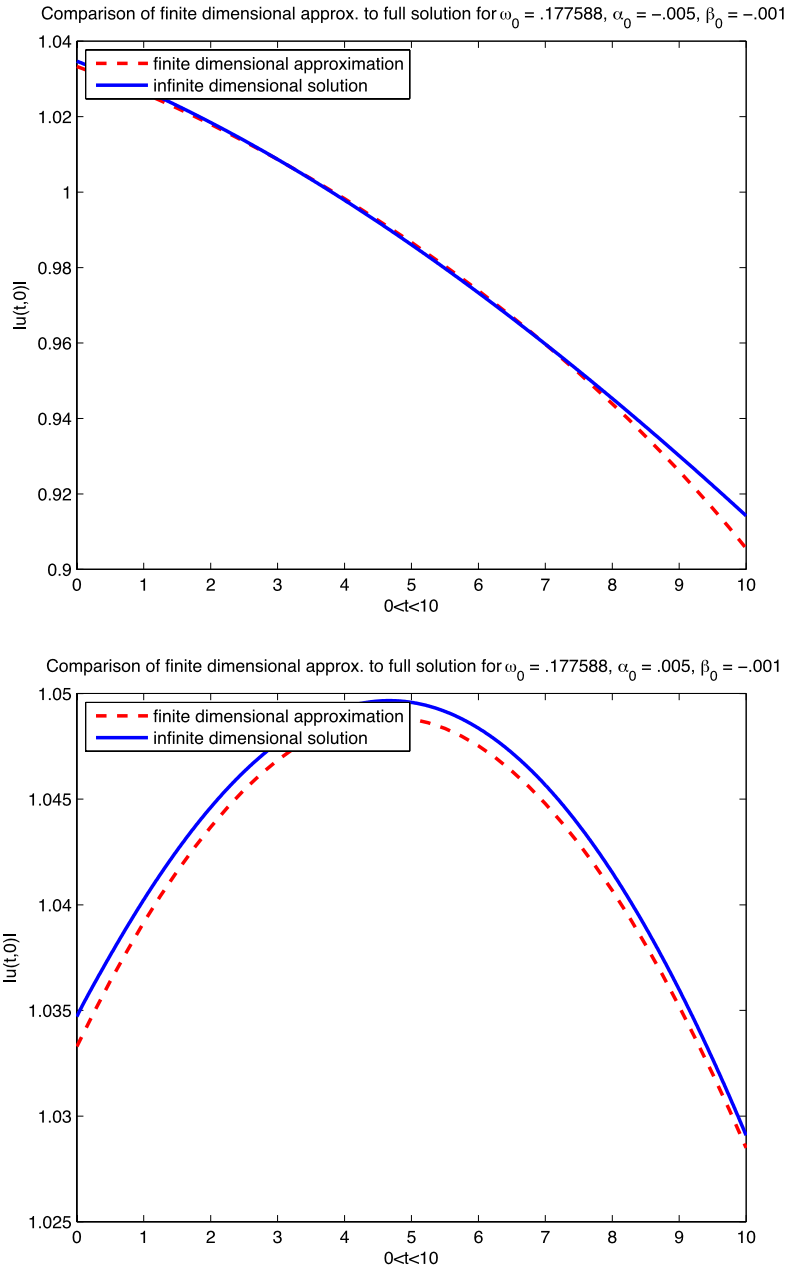

Fig. 6 A plot of the solution to the system of ODE's as well as the full solution to (1.1) derived for solutions near the minimal soliton for $\alpha_0 = \rho_3(0) > 0$ and $\alpha_0 = \rho_3(0) < 0$, $\beta_0 = \rho_4(0) < 0$ for $\omega_0 = 0.177588$, $N = 1000$

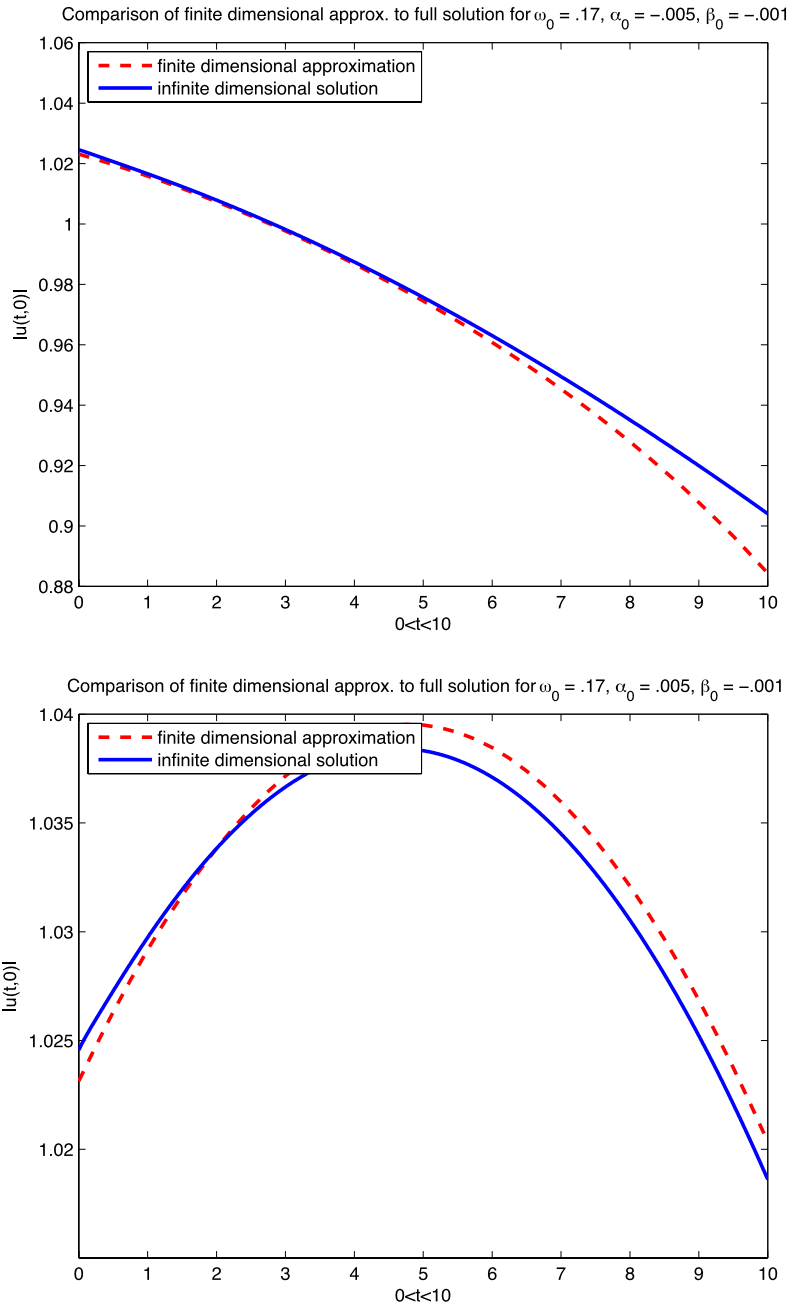

Fig. 7 A plot of the solution to the system of ODE's as well as the full solution to (1.1) derived for solutions near the minimal soliton for $\alpha_0 = \rho_3(0) > 0$ and $\alpha_0 = \rho_3(0) < 0$, $\beta_0 = \rho_4(0) < 0$ for $\omega_0 = 0.17$, $N = 500$

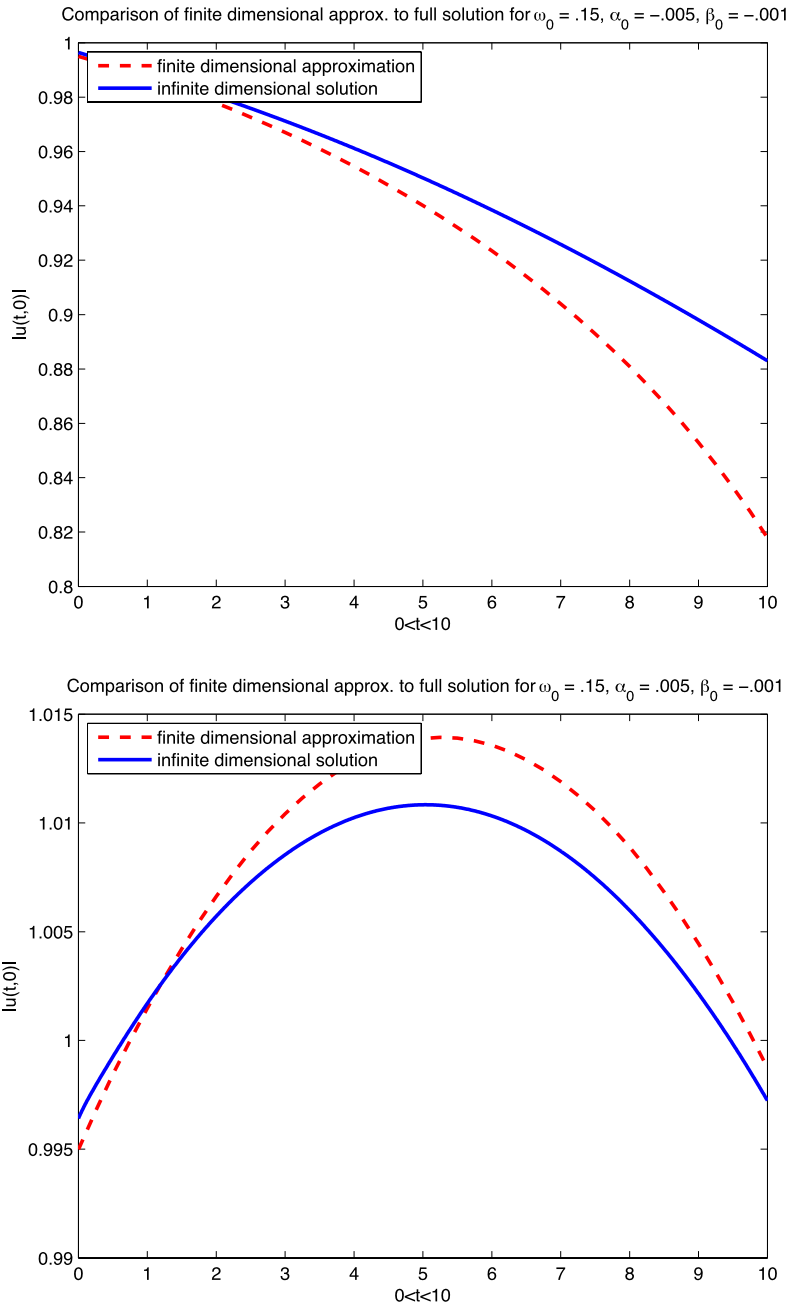

Fig. 8 A plot of the solution to the system of ODE's as well as the full solution to (1.1) derived for solutions near the minimal soliton for $\alpha_0 = \rho_3(0) > 0$ and $\alpha_0 = \rho_3(0) < 0$, $\beta_0 = \rho_4(0) < 0$ for $\omega_0 = 0.15$, $N = 500$

the primitive system. Obviously, we eventually leave the regime of validity for our approximation. But it is notable that on the shorter time scales, our system captures some aspect of the full dynamics.

We cannot numerically verify our conjecture that soliton-preserving perturbations of unstable solitons dynamically select stable solitons. However, when we begin with perturbations that are expected to continue to have a soliton component, we see oscillations about the minimal mass; this strongly suggests that, through coupling to the continuous spectrum, the oscillations will damp toward a near-minimal-mass stable soliton. This would be quite satisfying from a physical perspective as the system would be moving toward the configuration of lowest energy in some sense.

Our ultimate objective is to rigorously characterize the stability properties of the minimal mass soliton. We conjecture that perturbations giving rise to oscillatory dynamics in the finite dimensional system will, in the primitive equation, transition to a stable soliton. Excess mass will be lost by radiation damping. Likely, using current techniques this analysis can only be truly done in a perturbative setting, though we also conjecture that initial conditions near strongly unstable solitons should exhibit similar behavior. Hopefully, more powerful techniques will eventually be developed for the global study of the stable soliton curve as an attractor of the full nonlinear dynamics.

Acknowledgements This project began out of a conversation with Catherine Sulem and JLM. JLM was partially funded by an NSF Postdoc at Columbia University and a Hausdorff Center Postdoc at the University of Bonn. In addition, JLM would like to thank the University of North Carolina, Chapel Hill for graciously hosting him during part of this work. SR would like to thank the University of Chicago for their hospitality while some of this work was completed. GS was funded in part by NSERC. In addition, the authors wish to thank Dmitry Pelinovsky, Mary Pugh, Catherine Sulem, and Michael Weinstein for helpful comments and suggestions.

Appendix A: Details of Numerical Methods

A.1 Sinc Approximation

Here, we briefly review sinc and its properties. The texts (Lund and Bowers 1992; Stenger 1993) and the articles (Stenger 1981, 2000; Bellomo 1997) provide an excellent overview. As noted, sinc collocation and Galerkin schemes have been used to solve a variety of partial differential equations.

Recall the definition of sinc,

$$\operatorname{sinc}(z) \equiv \begin{cases} \frac{\sin(\pi z)}{\pi z}, & \text{if } z \neq 0, \\ 1, & \text{if } z = 0, \end{cases} \tag{A.1}$$

and for any $k \in \mathbb{Z}$, $h > 0$, let

$$S(k,h)(x) = \operatorname{sinc}\left(\frac{x - kh}{h}\right). \tag{A.2}$$

The sinc function can be used to exactly represent functions in the Paley–Wiener class. We spectrally represent functions with sinc in a weaker function space. First, we define a *strip* in the complex plane,

$$D_d = \{z \in \mathbb{C} \mid |\mathrm{Im}\, z| < d\}. \tag{A.3}$$

We work in the following function space.

Definition A.1 $B^p(D_d)$ is the set of analytic functions on D_d satisfying:

$$\left\| f(t + \mathrm{i}\cdot) \right\|_{L^1(-d,d)} = O\left(|t|^a\right), \quad \text{as } t \to \pm\infty, \text{ with } a \in [0, 1), \tag{A.4a}$$

$$\lim_{y \to d^-} \left\| f(\cdot + \mathrm{i}y) \right\|_{L^p} + \lim_{y \to d^-} \left\| f(\cdot - \mathrm{i}y) \right\|_{L^p} < \infty. \tag{A.4b}$$

Then we have the following theorem.

Theorem A.1 (Theorem 2.16 of Lund and Bowers 1992) *Assume* $f \in B^p(D_d)$, $p = 1$ *or* 2, *and* f *satisfies the decay estimate*

$$\left| f(x) \right| \leq C \mathrm{e}^{-\alpha |x|}. \tag{A.5}$$

If h *is selected such that*

$$h = \sqrt{\pi d/(\alpha M)} \leq \min\{\pi d, \pi/\sqrt{2}\}, \tag{A.6}$$

then

$$\left\| \partial_x^n f - \partial_x^n C_M(f, h) \right\|_{L^\infty} \leq C M^{(n+1)/2} \mathrm{e}^{((-\sqrt{\pi d \alpha M}))}.$$

d identifies a strip in the complex plane, of width $2d$, about the real axis in which f is analytic. An appropriate choice of this parameter may not be obvious; others have found $d = \pi/2$ sufficient.

For the NLS equation of order $2\sigma + 1$,

$$d_{\mathrm{NLS}} = \frac{\pi}{\sqrt{2\omega\sigma}}.$$

Saturated NLS "interpolates" between second and seventh order NLS. We thus reason that it is fair to take $d = \pi/\sqrt{6\omega}$. Though we do not prove that the soliton and the associated elements of the kernel lie in these $B^p(D_d)$ spaces or satisfy the hypotheses of Theorem A.1, we use (A.6) to guide our selection of an optimal h. Since the soliton has $\alpha = \sqrt{\omega}$, we reason that it should be acceptable to take

$$h = \sqrt{\frac{\pi d}{\alpha M}} = \sqrt{\frac{\pi^2}{6\omega M}}. \tag{A.7}$$

(A.7) is dependent on both M and ω. Were we to use (A.7) as is, it would complicate approximating, amongst other things, the derivative with respect to ω of the soliton.

To avoid this, we use a priori estimates on ω^*, given in Appendix A.4.1. Since we know that $\omega^* \sim 0.18 < 0.25$, it is sufficient to take

$$d = \pi\sqrt{2/3}.$$

Likewise, since $\omega^* > 0.1$, we may take

$$\alpha = \sqrt{1/10}.$$

Thus, instead of (A.7), we use

$$h = \pi\sqrt{\frac{\sqrt{20/3}}{M}}. \tag{A.8}$$

We conjecture that this is a valid grid spacing for all $\omega \in (0.1, 0.25)$; our computations are consistent with this assumption.

A.2 Numerical Continuation

As discussed in Sect. 4.1, the discrete system approximating (1.5) is

$$\vec{F}(\vec{\phi}) = D^{(2)}\vec{\phi} - \omega\vec{\phi} + g(\vec{\phi})\vec{\phi} = 0. \tag{A.9}$$

The multiplication in $g(\vec{\phi})\vec{\phi}$ is performed elementwise. In order to solve this discrete system, we need a good starting point for our nonlinear solver. We produce this guess by numerical continuation.

Define the function

$$\hat{g}(x;\tau) = \frac{x^3}{1+\tau x^2}.$$

Note that $\hat{g}(x,0)$ is 7th order NLS and $\hat{g}(x,1) = g(x)$, saturated NLS. We now solve

$$\vec{G}(\vec{\phi};\tau) = D^{(2)}\vec{\phi} - \lambda\vec{\phi} + \hat{g}(\vec{\phi};\tau)\vec{\phi} = 0. \tag{A.10}$$

At $\tau = 0$, the analytic NLS soliton serves as the initial guess for computing $\vec{\phi}_{\tau=0}$. $\vec{\phi}_{\tau=0}$ is then the initial guess for solving (A.10) at $\tau = \Delta\tau$. We iterate in τ until we reach $\tau = 1$. This is numerical continuation in the artificial parameter τ, (Allgower and Georg 1990). This process succeeds with relatively few steps of $\Delta\tau$; in fact only $O(10)$ steps are required.

A.3 Convergence Data

Table 2 offers some examples of the robust and rapid convergence seen in the coefficients of (3.9). These values are all computed at the minimal mass soliton; also see Table 1.

Table 2 The convergence of several coefficients for the ODE system, computed at ω^*

M	a_0	$c14$	$p13$	$n133$
20	−0.54851448504	6.04829942099	−6.04829942099	8.79376331231
40	−0.553577138662	6.12521927361	−6.12521927361	8.81625889017
60	−0.553555163933	6.12811479039	−6.12811479039	8.81709463059
80	−0.553550441653	6.12827391288	−6.12827391288	8.81713847275
100	−0.553549989603	6.12828576495	−6.12828576495	8.81714173314
200	−0.553549934797	6.12828700415	−6.12828700415	8.81714206225
300	−0.553549934793	6.12828700423	−6.12828700423	8.81714206227
400	−0.553549934795	6.12828700421	−6.12828700421	8.81714206223
500	−0.553549934794	6.12828700423	−6.12828700423	8.81714206227

Table 3 The value of the coefficients in (3.9) computed with $M = 200$

Coefficient	Value
g_{33}	−6.61999411752
g_{44}	−12.4582451458
c_{14}	6.12828700415
c_{23}	1.46358108488
c_{34}	4.0422919871
c_{43}	0.131304385722
p_{13}	−6.12828700415
p_{24}	−17.9305799071
p_{33}	6.61999411752
p_{44}	12.4582451458
n_{133}	8.81714206225
n_{144}	1.84068246508
n_{234}	1.45559877602
n_{333}	−0.792198288158
n_{344}	0.013887281387
n_{434}	−0.0822482271619
a_0	−0.553549934797

A.4 Comparisons with Other Methods

We can benchmark our sinc algorithm against several other methods. Available algorithms include numerical quadrature along with more recent approaches such as spectral renormalization, also called the Petviashvili method (Petviashvili 1976; Ablowitz and Musslimani 2005; Lakoba and Yang 2007), the imaginary time method (Bao and Du 2004; Yang and Lakoba 2008), and the squared operator method (Yang and Lakoba 2007).

A.4.1 Quadrature Methods

The soliton equation may be integrated once to get

$$\frac{1}{2}(\partial_x\phi)^2 - \frac{1}{2}\lambda\phi^2 + \frac{1}{4}\left[\phi^4 - \log\left(1+\phi^4\right)\right] = 0. \tag{A.11}$$

Equation (A.11) yields an implicit algebraic expression for the amplitude, $\phi(0)$,

$$-\frac{1}{2}\lambda\phi(0)^2 + \frac{1}{4}\left[\phi(0)^4 - \log\left(1+\phi(0)^4\right)\right] = 0. \tag{A.12}$$

Using (A.11) and (A.12), we can express the mass as

$$\begin{aligned}\|\phi\|_{L^2}^2 &= \int_{-\infty}^{\infty}\phi(x)^2\,\mathrm{d}x = 2\int_0^{\infty}\phi(x)^2\,\mathrm{d}x \\ &= 2\int_0^{\phi(0)}\rho^2\left\{\lambda\rho^2 - \frac{1}{2}\left[\rho^4 - \log\left(1+\rho^4\right)\right]\right\}^{-1/2}\mathrm{d}\rho.\end{aligned}$$

Thus, the mass of the soliton with parameter ω is

$$\|\phi_\omega\|_{L^2}^2 = 2\int_0^{\phi(0;\omega)}\rho^2\left\{\omega\rho^2 - \frac{1}{2}\left[\rho^4 - \log\left(1+\rho^4\right)\right]\right\}^{-1/2}\mathrm{d}\rho. \tag{A.13}$$

Equations (A.12) and (A.13) can be used to approximate ω^* by numerically minimizing (A.13). To compute the amplitude of the soliton, we solve (A.12) using Brent's method with a tolerance of 1.0e–14. We use the singular integral integrator QAGS from QUADPACK, which for this problem is, unfortunately, limited to a relative error of 5.0e–12 and an absolute error of 1.0e–15. Trying different routines from the optimization module of SciPy, (Jones et al. 2001), we summarize our results in Table 4, which contains data from our sinc computations. There is a spread of O(1e–12) amongst the computed minimal masses and a spread of O(1e–7) amongst the ω^*. These differences are consistent with the prescribed relative error of the quadrature,

Table 4 The soliton parameter and mass of the minimal mass soliton computed by several methods, including both quadrature and spectral renormalization. Also included is some of the data for the sinc method which appeared in Table 1

Algorithm	ω^*	$\int \lvert\phi\rvert^2\,\mathrm{d}x$
fminbound	0.177588368745261	3.821149022780204
Brent	0.177587963826864	3.821149022778472
golden	0.177587925853761	3.821149022776717
Spec. Re.	0.177588064106709	3.821149022780361
sinc with $M = 100$	0.177588063805561	3.821149022493814
sinc with $M = 200$	0.177588065432740	3.821149022780618
sinc with $M = 400$	0.177588065433095	3.821149022780896

suggesting the precision of this approach to computing the minimal mass and associated ω is limited by the quadrature algorithm. Note that we do not compute the solitary wave with this technique; we merely identify the minimal mass soliton parameter and the mass of that soliton.

A.4.2 Spectral Renormalization Methods

A Fourier transform may be applied to the soliton equation to get

$$\hat{\phi_\omega}(k) = \frac{\mathcal{F}(g(\phi_\omega^2)\phi_\omega)(k)}{k^2+\omega} \tag{A.14}$$

where k is the wave number. Let us introduce variable $w(x)$, with $\phi_\omega(x) = \theta w(x)$,where θ is an unknown, nonzero, constant. Introducing this into (A.14), we have

$$\hat{w}(k) = \frac{\mathcal{F}(g(\theta^2 w^2)w)(k)}{k^2+\omega} \equiv \mathcal{Q}_\theta[\hat{w}](k). \tag{A.15}$$

Multiplying (A.15) by $\hat{w}(k)^*$, the complex conjugate, and integrating over all k, we compute

$$G(\theta;\hat{w}) \equiv \int |\hat{w}(k)|^2 \,\mathrm{d}k - \int \hat{w}(k)^* \mathcal{Q}_\theta[\hat{w}](k)\,\mathrm{d}k = 0. \tag{A.16}$$

This may be interpreted as a constraint on θ. This motivates the iteration described in Ablowitz and Musslimani (2005). Suppose we know $w_m(x)$ and θ_m, a pair of approximations of the true values. To get the next approximation, we compute

$$\hat{w}_{m+1}(k) = \mathcal{Q}_{\theta_m}[\hat{w}_m](k) \tag{A.17}$$

and then solve

$$G(\theta;\hat{w}_{m+1}) = 0 \tag{A.18}$$

for θ_{m+1}. We repeat this until the sequence $\{w_m\}$ satisfies our convergence criteria. From this, we then recover ϕ_ω. The advantage of this method is that one can use the fast Fourier transform. Using spectral renormalization, we then minimize the approximate mass numerically. This is readily implemented in MATLAB, using `fzero` to solve (A.18) for a given value of ω and `fminbnd` to find the minimal mass value of ω. We iterate in w until either $\|w_{m+1} - w_m\|_{\ell^2} <$ Abs. Tol. or $\|w_{m+1} - w_m\|_{\ell^2}/\|w_{m+1}\|_{\ell^2} <$ Rel. Tol. This is performed with a relative and absolute tolerances of 1e–15 in the spectral renormalization component, and a tolerance of 1e–15 in both `fminbnd` and `fzero`. Our spatial domain is $[-200, 200)$ with 2^{12} grid points. As seen in Table 4, this is in good agreement with both the sinc method and the quadrature method.

References

Ablowitz, M.J., Musslimani, Z.H.: Spectral renormalization method for computing self-localized solutions to nonlinear systems. Opt. Lett. **30**(16), 2140–2142 (2005)

Akrivis, G., Dougalis, V., Karakashian, O., McKinney, W.: On fully discrete Galerkin methods of second-order temporal accuracy for the nonlinear Schrödinger equation. Numer. Math. **59**(194), 31–53 (1991)

Akrivis, G., Dougalis, V., Karakashian, O., McKinney, W.: Solving the systems of equations arising in the discretization of some nonlinear p.d.e's by implicit Runge–Kutta methods. RAIRO Modél. Math. Anal. Numér. **31**(3), 251–288 (1997)

Akrivis, G., Dougalis, V., Karakashian, O., McKinney, W.: Numerical approximation of blow-up of radially symmetric solutions of the nonlinear Schrödinger equation. SIAM J. Sci. Comput. **25**(1), 186–212 (2003)

Al-Khaled, K.: Sinc numerical solution for solitons and solitary waves. J. Comput. Appl. Math. **130**(1–2), 283–292 (2001)

Allgower, E.L., Georg, K.: Numerical Continuation Methods: An Introduction. Springer, Berlin (1990)

Bao, W., Du, Q.: Computing the ground state solution of Bose–Einstein condensates by a normalized gradient flow. SIAM J. Sci. Comput. **25**, 1674–1697 (2004)

Barashenkov, I.V., Panova, E.Y.: Stability and evolution of the quiescent and travelling solitonic bubbles. Physica D **69**, 114–134 (1993)

Barashenkov, I.V., Gocheva, A.D., Makhankov, V.G., Puzynin, I.V.: Stability of the soliton-like "bubbles". Physica D **34**, 240–254 (1989)

Bellomo, N.: Nonlinear models and problems in applied sciences from differential quadrature to generalized collocation methods. Math. Comput. Model. **26**(4), 13–34 (1997)

Bellomo, N., Ridolfi, L.: Solution of nonlinear initial-boundary value problems by sinc collocation-interpolation methods. Comput. Math. Appl. **29**(4), 15–28 (1995)

Berestycki, H., Lion, P.L.: Nonlinear scalar field equations, I: existence of a ground state. Arch. Ration. Mech. Anal. **82**(4), 313–345 (1983)

Bialecki, B.: Sinc-type approximations in H 1-norm with applications to boundary value problems. J. Comput. Appl. Math. **25**(3), 289–303 (1989)

Bialecki, B.: Sinc-collocation methods for two-point boundary value problems. IMA J. Numer. Anal. **11**(3), 357–375 (1991)

Boyd, J.P.: Chebyshev and Fourier Spectral Methods. Courier Dover, New York (2001)

Buslaev, V., Grikurov, V.: Simulation of instability of bright solitons for NLS with saturating nonlinearity. Math. Comput. Simul. 539–546 (2001)

Buslaev, V.S., Perelman, G.S.: On the stability of solitary waves for nonlinear Schrödinger equations. Am. Math. Soc. Transl. Ser. 2 **164**(1), 75–98 (1995)

Carlson, T.S., Dockery, J., Lund, J.: A sinc-collocation method for initial value problems. Math. Comput. **66**(217), 215–235 (1997)

Cazenave, T.: Semilinear Schrodinger Equations. Courant Lecture Notes in Mathematics, vol. 10. American Mathematical Society, Providence (2003)

Comech, A., Pelinovsky, D.: Purely Nonlinear Instability of Standing Waves with Minimal Energy. Commun. Pure Appl. Math. **56**, 1565–1607 (2003)

Cuccagna: On asymptotic stability of ground states of NLS. Rev. Math. Phys. **15**(8), 877–903 (2003)

Demanet, L., Schlag, W.: Numerical verification of a gap condition for a linearized nonlinear Schrödinger equation. Nonlinearity 829–852 (2006)

Dimitrevski, K., Reimhult, E., Svensson, E., Öhgren, A., Anderson, D., Berntson, A., Lisak, M., Quiroga-Teixeiro, M.L.: Analysis of stable self-trapping of laser beams in cubic-quintic nonlinear media. Phys. Lett. A **248**, 369–376 (1998)

Eisner, A., Turkington, B.: Nonequilibrium statistical behavior of nonlinear Schrödinger equations. Physica D **213**, 85–97 (2006)

El-Gamel, M.: Sinc and the numerical solution of fifth-order boundary value problems. Appl. Math. Comput. **187**(2), 1417–1433 (2007)

El-Gamel, M., Zayed, A.I.: Sinc-Galerkin method for solving nonlinear boundary-value problems. Comput. Math. Appl. **48**(9), 1285–1298 (2004)

El-Gamel, M., Behiry, S.H., Hashish, H.: Numerical method for the solution of special nonlinear fourth-order boundary value problems. Appl. Math. Comput. **145**(2–3), 717–734 (2003)

Erdogan, B., Schlag, W.: Dispersive estimates for Schrödinger operators in the presence of a resonance and/or eigenvalue at zero energy in dimension three. II. J. Anal. Math. **99**, 199–248 (2006)

Grillakis, M., Shatah, J., Strauss, W.: Stability theory of solitary waves in the presence of symmetry. ii. J. Funct. Anal. **94**(2), 308–348 (1990)

Holmer, J., Marzuola, J., Zworski, M.: Soliton splitting by external delta potentials. J. Nonlinear Sci. **17**(4), 349–367 (2007)

Johnston, T.W., Vidal, F., Fréchette, D.: Laser-plasma filamentation and the spatially periodic nonlinear Schrödinger equation approximation. Phys. Plasmas **4**(5), 1582–1588 (1997)

Jones, E., Oliphant, T., Peterson, P., et al.: SciPy: open source scientific tools for Python (2001)
Josserand, C., Rica, S.: Coalescence and droplets in the subcritical nonlinear Schrödinger equation. Phys. Rev. Lett. **78**(7), 1215–1218 (1997)
Josserand, C., Pomeau, Y., Rica, S.: Cavitation versus vortex nucleation in a superfluid model. Phys. Rev. Lett. **75**(17), 3150–3153 (1995)
Krieger, J., Schlag, W.: Stable manifolds for all monic supercritical focusing nonlinear Schrödinger equations in one dimension. J. Am. Math. Soc. **19**(4), 815–920 (2006)
Lakoba, T.I., Yang, J.: A generalized Petviashvili iteration method for scalar and vector Hamiltonian equations with arbitrary form of nonlinearity. J. Comput. Phys. **226**(2), 1668–1692 (2007)
LeMesurier, B.J., Papanicolaou, G., Sulem, C., Sulem, P.-L.: Focusing and multi-focusing solutions of the nonlinear Schrödinger equation. Physica D **31**(1), 78–102 (1988)
Lund, J., Bowers, K.L.: Sinc Methods for Quadrature and Differential Equations. Society for Industrial Mathematics, Philadelphia (1992)
Lundin, L.: A cardinal function method of solution of the equation $\Delta u = u - u^3$. Math. Comput. **35**(151), 747–756 (1980)
Marzuola, J., Simpson, G.: Spectral analysis for matrix Hamiltonian operators (2010, submitted). arXiv: 1003.2474
McCleod, K.: Uniqueness of positive radial solutions of $\Delta u + f(u) = 0$ in $\mathbb{R}^n$, II. Trans. Am. Math. Soc. **339**(2), 495–505 (1993)
Mohsen, A., El-Gamel, M.: On the Galerkin and collocation methods for two-point boundary value problems using sinc bases. Comput. Math. Appl. **56**(4), 930–941 (2008)
Pelinovsky, D.E., Afanasjev, V.V., Kivshar, Y.S.: Nonlinear theory of oscillating, decaying, and collapsing solitons in the generalized nonlinear Schrödinger equation. Phys. Rev. E **53**(2), 1940–1953 (1996)
Petviashvili, V.I.: Equation of an extraordinary soliton. Sov. J. Plasma Phys. **2**, 469–472 (1976)
Quiroga-Teixeiro, M., Michinel, H.: Stable azimuthal stationary state in quintic nonlinear optical media. J. Opt. Soc. Am. B **14**(8), 2004–2009 (1997)
Revelli, R., Ridolfi, L.: Sinc collocation-interpolation method for the simulation of nonlinear waves. Comput. Math. Appl. **46**(8–9), 1443–1453 (2003)
Rodnianski, I., Schlag, W., Soffer, A.: Asymptotic stability of N-soliton states of NLS. Preprint (2003)
Schlag, W.: Stable manifolds for an orbitally unstable nonlinear Schrödinger equation. Ann. Math. **169**(1), 139–227 (2009)
Shatah, J.: Stable standing waves of nonlinear Klein–Gordon equations. Commun. Math. Phys. **91**, 313–327 (1983)
Shatah, J.: Unstable ground state of nonlinear Klein–Gordon equations. Trans. Am. Math. Soc. **290**(2), 701–710 (1985)
Shatah, J., Strauss, W.: Instability of nonlinear bound states. Commun. Math. Phys. **100**, 173–190 (1985)
Soffer, A., Weinstein, M.I.: Resonances, radiation damping and instability in Hamiltonian nonlinear wave equations. Invent. Math. **136**(1), 9–74 (1999)
Stenger, F.: A "Sinc-Galerkin" method of solution of boundary value problems. Math. Comput. 85–109 (1979)
Stenger, F.: Numerical methods based on the Whittaker cardinal, or sinc functions. SIAM Rev. **23**, 165–224 (1981)
Stenger, F.: Numerical Methods Based on Sinc and Analytic Functions. Springer, Berlin (1993)
Stenger, F.: Summary of sinc numerical methods. J. Comput. Appl. Math. **121**(1–2), 379–420 (2000)
Sulem, C., Sulem, P.: The Nonlinear Schrödinger Equation. Self-Focusing and Wave-Collapse. Applied Mathematical Sciences, vol. 39. Springer, Berlin (1999)
Tikhonenko, V., Christou, J., Luther-Davies, B.: Three dimensional bright spatial soliton collision and fusion in a saturable nonlinear medium. Phys. Rev. Lett. **76**(15), 2698–2701 (1996)
Weinstein, M.I.: Modulational stability of ground states of nonlinear Schrödinger equations. SIAM J. Math. Anal. **16**, 472–491 (1985)
Weinstein, M.I.: Lyapunov stability of ground states of nonlinear dispersive evolution equations. Commun. Pure Appl. Math. **39**, 472–491 (1986)
Wright, E.M., Lawrence, B.L., Torruellas, W., Stegeman, G.: Stable self-trapping and ring formation in polydiacetylene para-toluene sulfonate. Opt. Lett. **20**(24), 2481 (1995)
Yang, J., Lakoba, T.I.: Universally-convergent squared-operator iteration methods for solitary waves in general nonlinear wave equations. Stud. Appl. Math. **118**(2), 153 (2007)
Yang, J., Lakoba, T.I.: Accelerated imaginary-time evolution methods for the computation of solitary waves. Stud. Appl. Math. **120**(3), 265–292 (2008)